International Journal for Uncertainty Quantification, 5 (1): 1–20 (2015)

MINIMAL SPARSE SAMPLING FOR FOURIER-POLYNOMIAL CHAOS IN ACOUSTIC SCATTERING

Roger M. Oba*

Acoustics Division, Naval Research Laboratory, Washington DC 20375, USA

Original Manuscript Submitted: 09/30/2013; Final Draft Received: 12/08/2014

Single frequency acoustic scattering from an uncertain surface (with sinusoidal components) admits an efficient Fourier-polynomial chaos (FPC) expansion of the acoustic field. The expansion coefficients are computed non-intrusively, i.e., by functional sampling from existing acoustic models. The structure of the acoustic decomposition permits sparse selection of FPC orders within the framework of the Smolyak construction. The main result shows a minimal, sparse sampling required to exactly reconstruct FPC expansions of Smolyak form. To this end, this paper defines two concepts: exactly discretizable orthonormal, function systems (EDO); and nested systems created by decimation or "fledging." An EDO generalizes the Nyquist-Shannon sampling conditions (exact recovery of "band-limited" functions given sufficient sampling) to multidimensional FPC expansions. EDO criteria replace the concept of polynomially exact quadrature. Fledging parallels the idea of sub-sampling for sub-bands, from higher to lower level. The FPC Smolyak construction is an EDO fledged from a full grid EDO. An EDO results exactly when the sampled FPC expansion can be inverted to find its coefficients. EDO fledging requires that the lower level (1) has grid points and expansion orders nested in the higher level, and (2) derives its map from the samples to the coefficients from the higher level map. The theory begins with a single dimension fledged EDO, since a tensor product of fledged EDOs yields a fledged tensor EDO. A sequence of nested EDO levels fledge recursively from the largest EDO. The Smolyak construction uses telescoping sums of tensor products up to a maximum level to develop nested EDO systems for sparse grids and orders. The Smolyak construction transform gives exactly the inverse of the weighted evaluation map, and that inverse has a condition number that expresses the numerical limitations of the Smolyak construction.

KEY WORDS: *Smolyak algorithm, polynomial chaos, stochastic sparse grid collocation, high-dimensional methods, stochastic partial differential equations, acoustics*

1. INTRODUCTION

Computational restrictions often enforce "good enough" approximation of uncertain physical properties, especially criterion when this involves deterministic computational models with random input. When the input consists of multidimensional, random, input parameters, minimal sampling becomes a major. At first glance, Nyquist-Shannon sampling notions for a regular grid would seem to incur the curse of dimensionality. Compressed sensing [1], however, finds many systems require much lower sampling rates, but may require a search for an acceptable system of representation. Additionally, many physical systems have exploitable properties that allow the use of the Smolyak construction [2] with sample sizes growing relatively slowly with dimension. The problem herein of acoustic random surface scattering represents such a system, with relatively weakly coupled parameters. In particular, the scattering problem has an efficient hybrid Fourier-polynomial chaos (FPC) representation of low order, but with many dimensions. The polynomial chaos (PC) theory rests upon approximating functions of random variables by sums of multidimensional

*Correspond to Roger M. Oba, E-mail: roger.oba@nrl.navy.mil

2152–5080/15/$35.00

orthogonal polynomials [3]. The random properties of the functions can then be rapidly computed by PC expansions, with examples in acoustics [4–7]. Finding the coefficients to the FPC expansion for the acoustic scattering problem uses functional evaluation from a numerical model for various input values of the random parameters on some part of a regular sampling grid, a non-intrusive PC method. The non-intrusive method finds the non-linear parameter dependence by linear computations. The expansions in this scattering case contain only terms typical of Smolyak expansions. The Smolyak construction can be adaptively refined until error estimates are small enough. Gerstner and Griebel [8] have extended the Smolyak construction to Gauss quadrature for PC coefficients. They base their method directly on the polynomially exact Gauss quadrature for each dimension. Each different order grid requires a new set of abscissas (sample points), a significant drawback for PC refinement since the function must be re-evaluated on the new grid. The use of the Patterson-Kronrod extension of Gauss abscissas [9] permits additional points which contain the previous grid set, allowing nesting. Unfortunately, the Patterson-Kronrod method for grid refinement may prove unsuitable. In particular, [10] shows that for Laguerre polynomials of degree larger than 3, the abscissas may include complex values not usable in standard underwater acoustic models. If, on the other hand, error estimates are known or previous calculations demonstrate convergence, then one may start with knowledge of the maximal quadrature or sampling grid required. Given the highest-order Gauss quadrature points, decimation of the grid could leave a nested sub-grid that can be used for sufficiently accurate functional approximation. This is the goal of this paper within the context of the acoustic scattering problem. As with many computational models, the smoothness properties of the computed acoustic fields are not well quantified, so error analysis will be done directly and not by function class (such as Korobov type, for example).

Compressed sensing offers an approach for sparse PC computations; e.g., see Doostan and Owhadi [11]. Consider a function represented by linear combination of a sparse set of orthonormal basis functions. The function evaluated at each point of sparse sampling grid can be accumulated into a vector-matrix equation. Following the example of compressed sensing, view the evaluation of the expansion as a linear mapping from basis coefficients to sampled values. An inverse of this map gives the coefficients computed from sample values of the function, and appropriate weighting vastly improves the condition number. The method described below for finding this inverse has a couple of advantages over the general compressed sensing method. Firstly, the physical problem itself often determines sparsity structure of the basis functions without further optimization. Secondly, this structure determines a minimal sampling grid that allows exact reconstruction for functions of interest. The latter fact derives the Nyquist-Shannon sampling theory and its equivalent for orthogonal functions. In Fourier analysis, continuous, finite-order ("band-limited") functions can be exactly computed from Fourier expansions determined by the coefficients. Conversely the coefficients can be found by continuous Fourier transform. The discrete Fourier transform (DFT) from functional evaluations over a sufficiently fine sampling grid (uniformly weighted and spaced) gives identical coefficients to the continuous transform. This allows exact recovery of the function from finite sampling. This holds even in higher dimensions, and the inverse DFT is simply the inverse of discretely sampled functional evaluation. The Nyquist-Shannon argument also holds for Gauss quadrature for computing PC coefficients for orthogonal polynomials and their tensor products. The Golub-Welsch method for Gauss quadrature weights and abscissas implicitly contains all the theory required. The FPC combines the PC and the Fourier theory.

The Smolyak construction, as viewed from Fourier analysis, considers multidimensional functions with particular smoothness properties, for example, Korobov or Nikol'skii class [12]. For these functions, the Fourier order and sampling can be sparsified immensely, and the discrete cosine transform exactly maps from the functional evaluation on sparse sampling onto the basis of sparse orders. The standard Smolyak construction typically considers only the zeroth-order (mean) quadrature, but in fact recovers other sparse-order coefficients, but Temirgaliev, Kudaibergenov, and Shomanova [13] have studied functional recovery for Fourier-Smolyak constructions. With the knowledge of the sparse orders, the inverse of evaluation of the Fourier expansion on a sparse grid can be computed directly and uses sparse transforms. The acoustic scattering problem propagates a periodic signal mediated by environment expressible by sums of periodic functions with random parameters. It represents a physical system where types of deterministic phenomena are generally known and largely understood. For this type of problem, compressed sensing will require at least as many samples as used here to approach the same accuracy, and will lose accuracy with fewer samples. In contrast, the compressed sensing usually involves poorly studied systems giving rise to matrices of unknown sparsity, but performs well in the face of minimal information [14].

In the Smolyak construction, the lower-order, polynomially exact Gauss quadrature for PC coefficients fails to have a nested grid. By taking a more algebraic approach, one can find alternative, smaller-order transforms with the identical order of standard Gauss quadrature, but which allow nesting. This requires defining a new measure of exactness, directed toward the goal of finding FPC coefficients. The fledging process provides nested sequences of systems, each meeting the new exactness criteria. The criteria will bootstrap from a single dimension into tensor products and ultimately into the Smolyak construction.

The story develops as follows: The next section outlines an acoustic scattering problem that has a FPC representation sufficiently approximated by Smolyak orders. The computations use legacy code sampled on hybrid Fourier-Gauss quadrature grids. Section 3 develops the required theory for fledging exactly discretizable orthonormal systems in one dimension. Definitions emphasize matrix methods for exact computation of integral inner products, allowing finite functional sampling to recover the original function, a special property shared by Fourier and PC decompositions. A theorem gives an equivalent property, which is then exploited to find nested systems with the same property. A Fourier example illustrates these ideas applied to a non-standard system from the acoustic problem. Section 4 begins by bootstrapping single dimension results into tensor product spaces, and retraces steps of Section 3. The last bit of theory is a telescoping sum that allows the definition of the Smolyak construction. The telescoping sum then assumes the same property of exact functional recovery. Finally, the acoustic problem returns as a basis for studying the errors incurred for the new Smolyak construction applied to a physical problem.

2. PRELIMINARIES

2.1 Notation and Indexing

Notation for multidimensionality, tensor products, functional order, sub-gridding, and so forth, will require some conventions. Each section will have its own indexing, and once a concept is developed, indexing becomes implicit, for example, "$\mathbf{Q}_{\lambda-1}$ is the fledged sub-matrix of $\mathbf{Q}_\lambda$." Where possible concepts will be developed in a single dimension. The sub- and super-scripting roughly follow Novak and Ritter [15]. Superscripts on variables will represent grid points (abscissas) "$\phi_j = F\left(\xi^j\right)$." An arbitrary dimension is "d" and the largest is "D." "P" represents an orthogonal function (polynomial or Fourier) and a superscript indicates order "P^k, $k = 0, 1, \ldots$." The notion of level indices will be indicated by a Greek subscript "$N_\lambda = 2^\lambda$ for $0 \le \lambda \le \Lambda$," with indexing starting with 0. Square brackets will indicate the individual component of a vector (lower case bold) or matrix (uppercase bold) "$[\mathbf{Q}_\lambda]_{jk}$." Linear transforms, especially those extended from a sub-space to the entire space, will be indicated by the corresponding italic capitals "$[\mathbf{Q}_\lambda]_{jk} = [Q_\lambda]_{g_j \chi_k}$." Multi-indices are bold, typically in sub- or superscripts "$P^{\mathbf{k}}\left(\xi^{\mathbf{j}}\right)$" or "$N_{\mathbf{\Lambda}}$." This paper will not distinguish Fourier components from polynomial, and implicitly $P^k(\xi) = e^{ik\xi}$, where $i = \sqrt{-1}$, $\xi \in [0, 2\pi)$ or an equivalent interval, and integer k may be negative. Another approach would be expressing Fourier terms as monomials on the unit circle $P^k(\xi) = \xi^k$, $|\xi| = 1$, $\xi \in \mathbb{C}$, which can be regarded as orthonormal with respect to the uniform distribution on the unit circle [16]. The more standard Fourier notation appears here, since no real use of orthogonal polynomials on the unit circle is required.

2.2 The Acoustical Problem

The example here revisits the problem of [17]: acoustic scattering from an undulating surface ensonified by an acoustic beam. A single frequency line source at range 0 m uses a Gaussian beam source

$$F_{\mathrm{T}}(z) = \exp\left[-(z - z_{\mathrm{s}})^2/\sigma^2\right] \exp\left[i\kappa \sin\theta\,(z - z_{\mathrm{s}})\,(1 + \Theta)\right],$$

where $z_{\mathrm{s}} = 66.12$ m is the mean source depth, $\sigma = 27.55$ m is effective source width, $\theta = 10^\circ$ the upward beam angle, and $\kappa = 2\pi/\lambda$ is the acoustic wavenumber with acoustic wavelength $\lambda = 3.75$ m. The Thorsos taper phase correction $\Theta = (2z^2 - \sigma^2)/(\kappa^2\sigma^2\cos^2\theta)$ helps maintain beam shape [18]. The model source achieves zero pressure at the top surface with a reflection term $F_{\mathrm{s}}(z) = F_{\mathrm{T}}(z) - F_{\mathrm{T}}(z + 2z_{\mathrm{s}} + 2h_{\mathrm{s}})$, where h_{s} is the uncertain surface height directly above the source. The beam is directed so that it impinges in the middle of variable height surface of 750 m horizontal extent. Other details of the acoustic propagation model (including surface flattening via conformal mapping) appear in [17].

Surface wave models commonly use complex Fourier components with random amplitudes with complex normal distribution. (Taking the real part gives surface height realizations.) This corresponds to exponential distribution of surface wave energy (proportional to amplitude squared) and uniformly distributed phases. Acoustic wave scattering from surface components shows strong resonance effects occurring at harmonics of the surface wavelengths according to Bragg scattering. If each surface wave Fourier component has uniformly distributed phase, the uncertain acoustic field separates into Fourier orders with respect to the surface wave phase identical to Bragg scattering orders. The corresponding exponential distribution of amplitude squared then drives the (normalized) Laguerre polynomials L_k, $k = 0, 1, ...$ paired with Fourier expansions of the acoustic field. Xiu and Shen [19] used physical space Fourier-Legendre expansions for acoustic scattering from rough cylinders. Their physical space expansion is analogous to the geometry considered here: in two-dimensions the form Helmholtz equation is invariant under conformal mapping, and the complex logarithm maps a closed curve to a periodic surface. To simplify presentation of results, this paper considers the case of a single wavelength surface. In this case, the two random parameters correspond to the phase, $0 \leq \xi_0 < 2\pi$, and the surface amplitude squared, $0 \leq \xi_1 < \infty$. The uncertain acoustic field $F(\xi_0, \xi_1; r, z,)$ is a function of range r and depth z, increasing downward. Then the acoustic field may be expressed as function of parameters by a Fourier-polynomial chaos (FPC) expansion

$$F(\xi_0, \xi_1) = F(\xi_0, \xi_1; r, z) = \sum_{j=-\infty}^{\infty} \sum_{k=0}^{\infty} c_{jk} \exp(2\pi i j \xi_0) L^k(\xi_1),$$

where $c_{jk} = c_{jk}(r, z)$ has the spatial dependence suppressed. Since all the discussion that follows applies for pointwise analysis, that is, for fixed choice of (r_0, z_0), neglecting spatial dependence will not cause ambiguity. After pointwise analysis, the results can be recombined to give range-depth plots that accumulate the spatial dependence of the coefficients c_{jk}. The plots of Fig. 1 show the pointwise results of Fourier-Laguerre coefficient computations, with

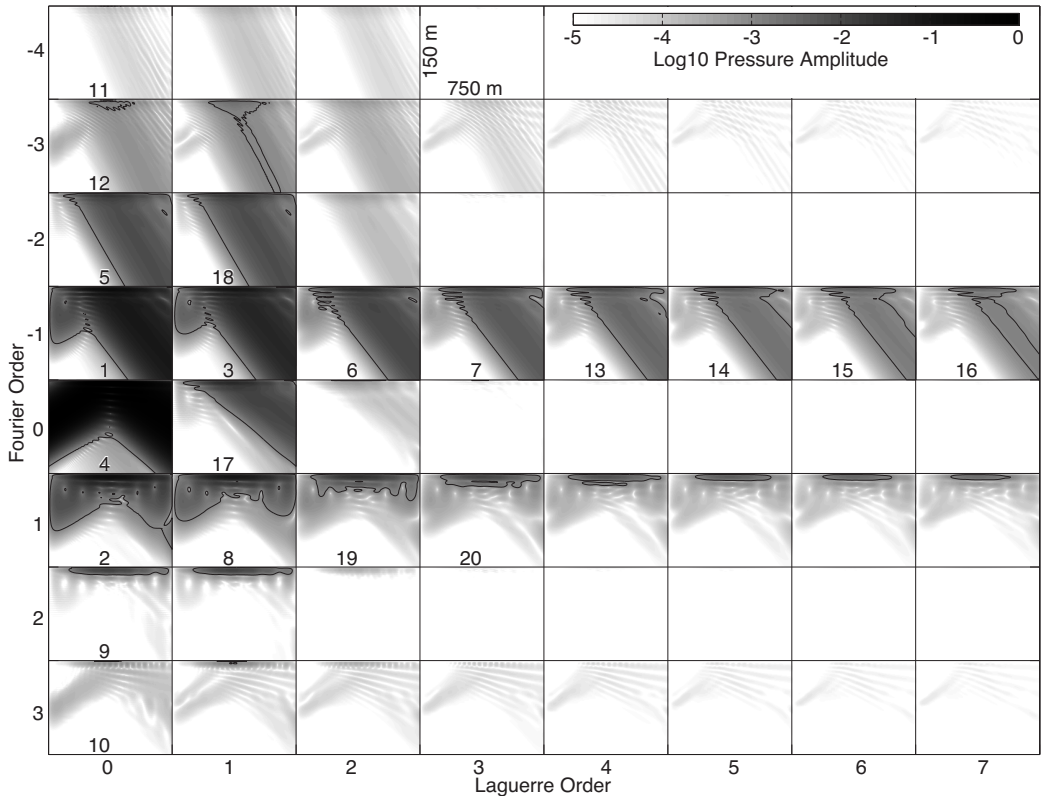

FIG. 1: Acoustic scattering Fourier-Laguerre decomposition.

each small frame exhibiting the spatial distribution of logarithm of the amplitude over a range of 750 m and depth of 150 m. The coefficient orders are shown along the outside of the large frame, Fourier orders vertically and Laguerre orders horizontally. The c_{00} frame shows the source on the left, beamed upward at the surface, and to the right, the mean specular reflection. Each row corresponds to a Bragg scattering order, coincident with the Fourier order. The actual computations use the Fourier transform with Laguerre-Gauss quadrature over $-8 \leq j \leq 7$ and $0 \leq k \leq 15$ to compute the acoustic field coefficients at each location. These differ from Fourier-Laguerre $-16 \leq j \leq 15$ by $0 \leq k \leq 31$ computations by 10^{-4}. The results for Fourier orders $-4 \leq j \leq 3$ and Laguerre orders $0 \leq k \leq 7$ shown here are sufficient to compute the acoustic field to two-significant figures accuracy (0.1 dB) at 750 m range appearing at the right edge of each plot. The ensonifying beam and its specular reflection dominate the mean Fourier term c_{00}. On the other hand, the Fourier (or Bragg) –1 order dominates all $k > 0$ contributions and is clearly non-linear in the Laguerre orders plotted here. The next dominant row for $k > 0$ is the Fourier order 1 followed by 0, –2, ... The main criteria include coefficients across all depths at 750 m range with amplitudes greater than 10^{-3} below the peak source level; this amplitude contour is indicated in each plot. In fact, the Laguerre order 9 coefficients (not shown) do fall below that level. The small frames with numbers are those included in a particular Smolyak construction and conform to the amplitude criteria. This excludes Fourier-Laguerre order (–3,1) which only meets the criteria at shorter ranges. This includes frames numbered 10–12 which fail to meet the criteria. Thus, the objective becomes to find a method using a sparse sampling grid that allows computation of the dominant terms in Fig. 1. Lastly, the hybrid Fourier-Laguerre representation can transform into a Hermite-Hermite representation corresponding to the original complex normal distribution; although this would be a true PC representation, it is not sparse.

3. EDO AND FLEDGED FUNCTION SYSTEMS OF ONE VARIABLE

The bulk of the heavy lifting follows in a single dimension to develop computational tools. The section starts with an example to motivate the main definition of EDO. This is then shown to be equivalent to inversion of a weighted evaluation matrix. Fledging becomes a matter of the relatively simple notion of finding invertible sub-matrices. Iterate fledging provides the backbone of a nested sequence of EDOs. Much of the theory relies on index bookkeeping of the grid decimation, and formally this is handled by projection operators. The technicalities, definitions, and structures follow the example:

Fourier example: Consider the complex exponentials $\mathbb{O} = \left\{e^{ik\xi} : \xi \in I,\, k \in \mathbb{Z}\right\}$, where $I = [0, 2\pi)$ and the integers, $\mathbb{Z}$, index the functions by Fourier orders. The functions are orthonormal with respect to uniform probability measure, a constant $\mu \equiv 1/2\pi : \int_I e^{-ij\xi} e^{ik\xi} \mu d\xi = \delta_{jk}$, the Kronecker delta. In practice, many functions on I have appropriate continuous band-limited approximations, where the order index becomes finite, say $X = \{-N,\, -N+2,\, \ldots,\, N-1\}$. In such a case, functional sampling on $\Xi = \{\xi_n : \xi_n = \pi n/N,\, n \in G\}$ with grid indices $G = \{0, 1, \ldots, 2N-1\}$ exactly determines the band-limited approximation via the DFT:

$$f(\xi) = \sum_{n \in X} c_n e^{in\xi},\; c_n = \int_I e^{-in\xi} f(\xi)\, \mu d\xi = \sum_{m \in G} e^{-in\xi_m} \tfrac{1}{2N} f(\xi_m), \tag{1}$$

for the linear span $\mathcal{L}(\mathbb{O}_X)$ of $\mathbb{O}_X = \left\{e^{ik\xi} : k \in \mathbb{O}\right\}$. In short, the finite discrete sum over the sampling grid exactly determines the continuous integral in (1). The weighted evaluation vector has components $[\boldsymbol{\phi}]_n = 1/\sqrt{2N}\, f(\xi_n)$, and $[\mathbf{c}]_n = c_n$. Then, the matrices mapping $\boldsymbol{\phi} = \mathbf{Q}\mathbf{c}$ have $[\mathbf{Q}]_{mn} = e^{in\xi_m}/\sqrt{2N}$. Inversely, $\mathbf{c} = \mathbf{R}\boldsymbol{\phi}$ has $\mathbf{R} = \mathbf{Q}^{-1}$ (with unitary $\mathbf{R} = \mathbf{Q}^{\dagger}$ and $\mathbf{Q}$, where † denotes conjugate transpose).

3.1 Definitions and EDO Theorem

An *orthonormal function system* written $(I,\, \mathbb{X},\, \mathbb{O},\, \mu)$ has an interval I and μ a probability measure on I. The *order* set $\mathbb{X}$ indexes the set of orthonormal functions $\mathbb{O}$ with respect to μ; i.e., if $P^j,\, P^k \in \mathbb{O}$ $(j,\, k \in \mathbb{X})$,

$$\int_I \bar{P}^j(\xi)\, P^k(\xi)\, \mu(\xi)\, d\xi = \delta_{j,k}, \tag{2}$$

with complex conjugation indicated by the over-bar, as necessary. Selection of a finite set $X \subset \mathbb{X}$, reduces the system to finite dimension, $N = N(X)$. For function F on I appropriate function space, the *truncation error* $\epsilon_X(\xi)$ is small for appropriate choice of X

$$F(\xi) = \sum_{j \in X} c_j P^j(\xi) + \epsilon_X(\xi). \tag{3}$$

The approach here develops computations algebraically, and numerical examples will revisit error estimates. Hence, in the following, consider the case $\epsilon_X \equiv 0$. In particular, take the continuous system $(I, X, \mathbb{O}_X, \mu)$ with finite dimensional set of order indices $X = \{\chi_1, \ldots, \chi_N\} \subset \mathbb{X}$ which determines $\mathbb{O}_X = \{P^j : P^j \in \mathbb{O} \text{ and } j \in X\}$. For function $f \in \mathcal{L}(\mathbb{O}_X)$, the linear span of $\mathbb{O}_X$,

$$f(\xi) = \sum_{\chi \in X} c_\chi P^\chi(\xi). \tag{4}$$

Integrals with orthonormal functions determine the coefficients, in operator form $\mathcal{P}_X : f \mapsto \mathbf{c} = [c_{\chi_1}, \ldots, c_{\chi_N}]$, as vectors, or componentwise

$$c_\chi = [\mathcal{P}_X f]_\chi = \int_I \bar{P}^\chi f(\xi)\, \mu(\xi)\, d\xi,\ \chi \in X. \tag{5}$$

A *discretization* $(G, X, \mathbf{R}, W)$ of an orthonormal system $(I, \mathbb{X}, \mathbb{O}, \mu)$ consists of the grid indices G for the sample points $\Xi \subset I$, a matrix $\mathbf{R}$, and weights W. The cardinalities of $G = \{g^1, \ldots, g^N\}$, X, and $W = \{w_1, \ldots, w_N\}$ must be the same $N = N(G) = N(X) = N(W)$, and $\mathbf{R}$ must be square of size $N \times N$. Consider $N = N(\Xi)$. [Later on, in Section 3.3, $N(G) < N(\Xi)$ requires fledging.] The *weighted evaluation* operator $\mathcal{E}_G$ simply creates a vector of values of a function at $\xi^k \in \Xi$, $k \in G$ and multiplies each component by $w_k \in W$, viz.,

$$\mathcal{E}_G f = \begin{bmatrix} w_1 f(\xi^1) \\ \vdots \\ w_N f(\xi^N) \end{bmatrix}. \tag{6}$$

Define $(G, X, \mathbf{R}, W)$ as an *exact discretization of an orthonormal* (EDO) system $(I, X, \mathbb{O}_X, \mu)$ if for $f \in \mathcal{L}(\mathbb{O}_X)$ a matrix multiplication gives the integral exactly:

$$c_\chi = [\mathbf{R}\mathcal{E}_\Xi f]_\chi = \int_I \bar{P}^\chi(\xi)\, f(\xi)\, \mu(\xi)\, d\xi. \tag{7}$$

The middle term of (7) reduces to the usual Gauss quadrature formula the appropriate W and Ξ.

Fourier example: Select $w_k = \sqrt{1/2N}$ and $\xi_k = \pi k/N$, where the weight w_k makes $\mathbf{R}$ unitary with $[\mathbf{R}]_{jk} = e^{-\pi i k j/2N}/\sqrt{2N}$. Equation (7) becomes exactly the DFT formula.

Because $\mathcal{L}(\mathbb{O}_X)$ is finite dimensional, the value of the c_χ exactly determines f by (4). This with (7) means finite sampling of f on Ξ exactly determines f on all of I. Also (7) can be written $c_\chi = [\mathbf{R}\mathcal{E}_G f]_\chi = [\mathcal{P}_X f]_\chi$, so that $\mathbf{R}\mathcal{E}_G = \mathcal{P}_X$ for EDO systems. Using (4) in (7), and linearity of $\mathcal{E}_G$ gives

$$c_\chi = \left[\mathbf{R} \sum_{j \in X} c_l \mathcal{E}_G P^l\right]_\chi = \sum_{j \in X} \sum_{k=1}^{N} [\mathbf{R}]_{\chi k}\, w_k P^j(\xi^k) c_j.$$

Because this holds for all $(I, X, \mathbb{O}_X, \mu)$, it means that the double sum on the right reduces to the Kronecker delta. Defining the matrix $\mathbf{Q}$ of weighted evaluation of the orthogonal functions,

$$[\mathbf{Q}]_{kl} = \left[\mathcal{E}_G P^l\right]_k = w_k P^l(\xi^k), \tag{8}$$

gives the main tool for EDO systems:

EDO theorem (in one dimension): $(I,\, X,\, \mathbb{O}_x,\, \mu)$ is an EDO with discretization $(G,\, X,\, \mathbf{R},\, W)$ if and only if $\mathbf{Q}$ is a weighted evaluation matrix for orthonormal functions as in (8) with

$$\mathbf{R} = \mathbf{Q}^{-1}. \tag{9}$$

Orthogonal polynomial examples: The theory of abscissas (functional sample grid), weights, as well as the exactness of Gauss quadrature (sometimes Gauss-Christoffel quadrature) with respect to a PDF $\mu(\xi)$ appear in Appendix A. In fact the notation of the previous sub-section derives from orthogonal polynomials in that P^j stands for polynomial, the w_k^2 are the (Christoffel) weights, and ξ^k are the (Christoffel) abscissas (the quadrature sample points). The matrix of terms $w_k P^j\left(\xi^k\right)$ are implicit in the Golub-Welsch method [20] as detailed by Gautschi in Chapter 1 of [21]. The details of interval, probability measure, and symmetric recursion matrix $\mathbf{J}$ (also called the Jacobi matrix) appear in Table 1.

The weights appear as eigenvalue norming constants and abscissas as eigenvalues of the tridiagonal matrix, with diagonal a_n and super- and sub-diagonal b_n for $n = 0, 1, \ldots$. When Ξ contains all eigenvalues and W the corresponding weights, $\mathbf{Q}$ and $\mathbf{R}$ are the matrices of left and right eigenvectors, respectively, and $\mathbf{R} = \mathbf{Q}^{\mathrm{T}}$.

3.2 Equivalent Vector Space Representations

The theory here relies on matrix manipulation between two vector spaces each equivalent to the original function space $f \in \mathcal{L}(\mathbb{O}_X)$, one with the objective of reconstruction and the other of sampling. From the *reconstruction* point of view, the space of coefficients C_X of the orthonormal function expansions (the FPC coefficients) has a bijection with the function space $\mathcal{L}(\mathbb{O}_X) \leftrightarrow C_X$: use (5) to map $f \mapsto \mathbf{c} = [c_1, \ldots, c_N]^{\mathrm{T}}$ and (4) for $\mathbf{c} \mapsto f$. From the *sampling* point of view, the vector space Φ_G of the weighted functional evaluations at the grid points relates to the function space $\mathcal{L}(\mathbb{O}_X) \leftrightarrow \Phi_G$; the forward direction by $f \mapsto \boldsymbol{\phi} = \left[w_1 f\left(\xi^1\right), \ldots, w_N f\left(\xi^N\right)\right]^{\mathrm{T}}$. The inverse map $\boldsymbol{\phi} \mapsto f$ results from the EDO theorem since $\mathbf{c} = \mathbf{R}\boldsymbol{\phi} \in C_X$ and substitution into (4) completes $\boldsymbol{\phi} \mapsto \mathbf{c} \mapsto f$. Thus the matrix multiplications $\mathbf{Q} :\ C_X \to \Phi_g$ and $\mathbf{R} :\ \Phi_g \to C_X$ are equivalent to weighted evaluation $\mathcal{E}_G :\ f \mapsto \boldsymbol{\phi}$, and integral orthonormal decomposition $\mathcal{P}_X :\ f \mapsto \mathbf{c}$, respectively. By orthonormality, the inner products of f of (4) and $h = \sum_{\chi \in X} d_\chi P^\chi$ are $\sum_\chi \bar{c}_\chi d_\chi = \int_I \bar{f}(\xi)\, h(\xi)\, \mu(\xi)\, d\xi = \langle f, h \rangle$. Let $\boldsymbol{\eta} = \mathcal{E}_G h$, then for EDO systems

$$\langle \mathbf{R}\boldsymbol{\phi}, \mathbf{R}\boldsymbol{\eta} \rangle_{\mathbb{C}^N} = \langle \mathcal{P}_X f, \mathcal{P}_X h \rangle_{\mathbb{C}^N} = \langle f, h \rangle_{L^2}, \tag{10}$$

where the first two inner products are the Euclidean one on $\mathbb{C}^N$ and the third is the integral L^2 inner product on I with probability measure μ. The map $f \mapsto \mathbf{c} = \mathbf{R}\boldsymbol{\phi} \in C_X$ exactly discretizes integral inner products. This extends to norms as well.

Theorem: (Exact functional recovery): If $f \in \mathcal{L}(\mathbb{O}_X)$, $(G,\, X,\, \mathbf{R},\, W)$ is an EDO of $(I,\, X,\, \mathbb{O}_x,\, \mu)$, then f is uniquely reconstructed by (4) with $\mathbf{c}$ given by (7). The norm is preserved, $\|\mathbf{c}\|_{\mathbb{C}^N} = \|f\|_{L^2}$.

The development of fledged subspaces use the equivalent spaces C_X for reconstructed (or approximate) functions and Φ_G for the functional sampling on the grid. By the by, $\mathbf{Q}$ and $\mathcal{E}_G$ do not recreate the integral norms generally, but will, if W and Ξ are complete sets of Gauss-Christoffel weights and abscissas, or follow the Fourier example above.

TABLE 1: Orthogonal polynomial

Family	Symbol	I	μ	$\langle\xi\rangle$	$\sigma(\xi)$	a_n	b_n
Hermite	He_n	$(-\infty, \infty)$	$(1/\sqrt{2\pi})e^{-\xi^2/2}$	0	1	0	$\sqrt{n+1}$
Legendre	P_n	$(-1, 1)$	$1/2$	0	$1/\sqrt{3}$	0	$(n+1)/\sqrt{4(n+1)^2-1}$
Chebyshev (2nd kind)	U_n	$(-1, 1)$	$2/\pi\sqrt{1-\xi^2}$	0	$1/2$	0	$1/2$
Laguerre	L_n	$[0, \infty)$	$e^{-\xi}$	1	1	$2n+1$	$n+1$

3.3 Fledged EDO Systems and Notation

In the remainder of this section, fix a largest grid Ξ and use a set of grid indices G to indicate subsets of $\{\xi_g : g \in G\} \subset \Xi$. G also indexes the rows of $\mathbf{Q}$ (and the columns of $\mathbf{R}$) and X the columns of $\mathbf{Q}$ (and the rows of $\mathbf{R}$). Consequently sub-matrices of $\mathbf{Q}$ are determined by sub-grid indices $G' \subset G$ for rows and order index subset $X' \subset X$. In what follows, EDO will often stand for the "exact discretization of an orthonormal" system, with the continuous system $(I,\, X,\, \mathbb{O}_X,\, \mu)$ fixed and implied, so that $(I,\, X',\, \mathbb{O}_{X'},\, \mu)$ will be implicit with the selection of X'. Define a fledged EDO $(G',\, X',\, \mathbf{R}',\, W')$ of $(G,\, X,\, \mathbf{R},\, W)$, written $(G',\, X',\, \mathbf{R}',\, W') \lessdot (G,\, X,\, \mathbf{R},\, W)$ if $X' \subset X$ and $G' \subset G$, $N' = N\,(X') = N\,(G')$, the weights $W' = \{w_g : g \in G'\} \subset W$, and $\mathbf{R}'$ is $N' \times N'$ matrix derived from $\mathbf{R}$. Define the *fledgling* indices as those removed for the primed system (the relative compliment): $G - G'$ and $X - X'$. The *nestling* indices remain, exactly G' and X'. The principle fledging result is

EDO fledging theorem (in one dimension): If $(G,\, X,\, \mathbf{R},\, W)$ is an EDO system with $\mathbf{Q} = \mathbf{R}^{-1}$, and given a subset of orders $X' = \{\chi_1,\, \ldots,\, \chi_{N'}\} \subsetneqq X$, there is a fledged EDO with $(G',\, X',\, \mathbf{R}',\, W')$, $G' = \{g_1,\, \ldots,\, g_{N'}\}$ and

$$\mathbf{R}' = (\mathbf{Q}')^{-1}\,, \tag{11}$$

where $[\mathbf{Q}']_{jk} = [\mathbf{Q}]_{g_j \chi_k}$ and $[W']_j = [W]_{g_j}$.

Proof: By the EDO theorem it is sufficient to show that for any choice of $X' \subset X$, there is some choice of $G' \subset G$, with $N\,(G') = N\,(X')$ such that $[\mathbf{Q}']_{jk} = [\mathbf{Q}]_{g\chi}$ and $\mathbf{Q}'$ is invertible. By induction, it suffices to show only the case $N\,(X') = N\,(X) - 1$. For ease of notation suppose $X = \{1, \ldots, N\}$ and $X' = \{1, \ldots, N-1\}$ (without loss of generality). Note the invertibility of $\mathbf{Q}$ means $\det(\mathbf{Q}) \neq 0$. The proof now proceeds by contradiction; i.e., suppose there is no invertible sub-matrix with columns determined by X'. This is the same as saying all minors matrices $\tilde{\mathbf{Q}}_{jN}$, $j = 1, \ldots, N$ have zero determinant (recalling $\tilde{\mathbf{Q}}_{jN}$ is obtained by "crossing out" the Nth column and jth row of $\mathbf{Q}$). But then $\det(\mathbf{Q}) = \sum_{j=1}^{N} (-1)^{N-j}\, [\mathbf{Q}]_{jN} \det\left(\tilde{\mathbf{Q}}_{jN}\right) = 0$, a contradiction.

Corollary: Let $X = G = \{1, ..., N\}$; $(G', X', \mathbf{R}', W') \lessdot (G, X, \mathbf{R}, W)$ if and only if $\left[(\mathbf{R}')^{-1}\right]_{jk} = w_{g_j} P^{\chi_k}(\xi^{g_j})$ and $[W']_j = [W]_{g_j}$.

Standard Fourier example: Consider the Fourier indices $X = \{-2,\, -1,\, 0,\, 1\}$ and grid $\xi^g = \pi g/2$, $g \in G = \{0,\, 1,\, 2,,\, 3\}$. The weight is uniform $w = 1/2$, and $\mathbf{Q}$, the weighted Fourier evaluation coefficient matrix, has $[\mathbf{Q}]_{g\chi} = (1/2)e^{\pi i g \chi/2}$. $\mathbf{R}$ is the matrix for the DFT, $[\mathbf{R}]_{\chi g} = (1/2)e^{-\pi i g \chi/2}$. The usual order reduction $X' = \{0,\, 1\}$ has the sub-sampling indices $G' = \{0,\, 2\}$.

Scattering Fourier example: Consider the Fourier system above, with X, G, $\mathbf{Q}$, w, and $\mathbf{R}$ as immediately above. For the acoustic scattering at higher Laguerre orders, the Fourier indices $X' = \{-1,\, 1\}$ dominate. The respective exponential vectors $1/2[1\ -i\ -1\ i]^{\mathrm{T}}$ and $1/2[1\ i\ -1\ -i]^{\mathrm{T}}$ are the second and fourth columns of $\mathbf{Q}$. They differ most at quarter wavelengths, suggesting sub-sampling indices $G' = \{0,\, 1\}$. Hence

$$\mathbf{Q}' = \frac{1}{2}\begin{bmatrix} 1 & 1 \\ -i & i \end{bmatrix},\ \mathbf{R}' = \begin{bmatrix} 1 & i \\ 1 & -i \end{bmatrix}. \tag{12}$$

The theorem says decimation can work from the highest level to the lowest level, with nesting preserved by transitivity. Levels λ will index this nesting from 0 to maximal level Λ. Specifically, $\lessdot$ is transitive, and index EDO systems with $\kappa < \lambda < \nu$ such that $(G_\kappa,\, X_\kappa,\, \mathbf{R}_\kappa,\, W_\kappa) \lessdot (G_\lambda,\, X_\lambda,\, \mathbf{R}_\lambda,\, W_\lambda)$ and $(G_\lambda,\, X_\lambda,\, \mathbf{R}_\lambda,\, W_\lambda) \lessdot (G_\nu,\, X_\nu,\, \mathbf{R}_\nu,\, W_\nu)$. Then $(G_\kappa,\, X_\kappa,\, \mathbf{R}_\kappa,\, W_\kappa) \lessdot (G_\nu,\, X_\nu,\, \mathbf{R}_\nu,\, W_\nu)$. Thus the above theorem gives nested systems in a top-down manner, from the finest sampling with the most orders to a singleton sample for single order. A bottom-up theorem would show that starting at a lower level and inserting an intermediate level also works; that is, given additional orders, new grid points can be included. In fact, the lowest-level order(s) may be selected first, and then intermediate levels inserted all the way up as needed, and made to optimize condition numbers for $\mathbf{R}_\lambda$.

EDO bottom-up fledging theorem: If $(G',\, X',\, \mathbf{R}',\, W') \lessdot (G,\, X,\, \mathbf{R},\, W)$. Given $\tilde{X} \supsetneqq X'$ there is $\tilde{G} \supsetneqq G'$ such that $(G',\, X',\, \mathbf{R}',\, W') \lessdot \left(\tilde{G},\, \tilde{X},\, \tilde{\mathbf{R}},\, \tilde{W}\right) \lessdot (G,\, X,\, \mathbf{R},\, W)$, where the $\tilde{\mathbf{R}}$ and $\tilde{W}$ satisfy the correct fledging relations in both directions.

The proof appears in Appendix B.

3.4 Examples of Fledged Gauss Quadrature Grid Indices

Set the number of initial quadrature points to $N_\Lambda = 2^\Lambda$ with orders $X_\lambda = \left\{0, \ldots, 2^\lambda - 1\right\}$. Given these X_λ in top-down fledging, the criteria for $G_{\lambda-1} \subset G_\lambda$ is to select grid sub-indices that maximize the condition number of sub-matrix $\mathbf{Q}_{\lambda-1}$ extracted from $\mathbf{Q}_\lambda$. This continues to level 1, where level 0 grid index for the larger of $[\mathbf{Q}_1]_{X_0}$ determines G_0. For the bottom-up method, the 2×2 matrix $\mathbf{Q}_1$ maximizes condition number for all such sub-matrices of $\mathbf{Q}_\Lambda$ for $X_1 = \{0, 1\}$. Then $\mathbf{Q}_{\lambda+1}$ is extracted from $\mathbf{Q}_\Lambda$ that maximizes condition number with the constraint that $G_{\lambda+1} \supset G_\lambda$. Note that the top level has condition number 1 since the discrete basis is orthonormal. Table 2 shows two examples of fledge gridding, one being top-down, the other bottom-up. Reading up from the bottom, level 1 shows which point is added to the 0 level point, and level 2 the points added to those below. The condition number is that of matrix with those grid indices and orders. Bottom-up fledging has a worse level 3 condition number but is slightly better at lower levels. In either case, the condition numbers give minimal increase in numerical error as the systems are fledged.

Scattering Fourier example: Set the top level indices $X_4 = \{-8, -7, \ldots, 7\}$ and $G_4 = \{0, 1, \ldots, 15\}$ for the computations of this paper. Orders indices are $X_0 = \{-1\}$, $X_1 = \{-1, 1\}$, $X_2 = \{-2, -1, 0, 1\}$, and $X_3 = \{-4, -3, \ldots, 3\}$. Set $G_0 = \{0\}$, without loss of generality; and use bottom-up fledging. With G_4 as above, $G_1 = \{0, 4\}$, and subsequently follows the standard DFT grid index selections $G_2 = \{0, 4, 8, 12\}$ and $G_3 = \{0, 2, \ldots, 14\}$. All condition numbers are 1.

3.5 Telescoping Matrices and Inversion

Part of the Smolyak construction requires the definition of telescoping sum of differences of transforms $\mathbf{R}_\lambda - \mathbf{R}_{\lambda-1}$, where $\mathbf{R}_\lambda = \mathbf{Q}_\lambda^{-1}$ fixes the matrix size. A formal issue first: the sub-matrix $\mathbf{R}_{\lambda-1}$ acts on a lower-dimensional subspace than $\mathbf{R}_\lambda$. In fact each level has a different dimensionality, and $\mathbf{R}_\lambda - \mathbf{R}_{\lambda-1}$ is ill defined as a linear map. This technicality captures the nature of fledged levels reducing the order and sampling simultaneously by sub-indexing. Projection operators (matrices) do the index bookkeeping in linear algebra. Delvos [22] previously used projections and their extensions for his construction.

3.5.1 Projection to Lower Level Grids and Orders

The projections defined here reduce dimension size from the Λ to λ levels for the equivalent vector spaces $\Pi_{X_\lambda} : C_\Lambda \to C_\lambda$ and $\Pi_{G_\lambda} : \Phi_\Lambda \to \Phi_\lambda$ of sub-section 3.2. As matrices the projections are of size $N_\lambda \times N_\Lambda$ constructed from the $N_\Lambda \times N_\Lambda$ identity matrix I_Λ by keeping only rows corresponding to X_λ or G_λ. The matrix definitions means $\Pi_{X_\lambda}^{\mathrm{T}} : C_\lambda \to C_\Lambda$ and $\Pi_{G_\lambda}^{\mathrm{T}} : \Phi_\lambda \to \Phi_\Lambda$ have the transpose matrix representations which embed the lower-dimensional

TABLE 2: One-dimensional Gauss-Laguerre fledging

Level	Top-down		Bottom-up	
	Add Pt ind	Cond #	Add Pt ind	Cond #
4	3, 6, 9, 11, 13-6	1	3, 7, 9, 12-6	1
3	1, 7, 10, 12	1.75	2, 5, 10, 11	2.24
2	4, 8	2.20	6, 8	1.87
1	5	1.18	4	1.10
0	2	1	1	1

vector spaces by using zeros for fledged orders or grid indices (respectively). Note that $\Pi_{X_\lambda}\Pi_{X_\lambda}^{\mathrm{T}} = \Pi_{G_\lambda}\Pi_{G_\lambda}^{\mathrm{T}} = I_\lambda$, the N_λ dimensional identity matrix. The operator $\left[\Pi_{X_\lambda}^{\mathrm{T}}\Pi_{X_\lambda}\mathbf{c}\right]_{jk} = [\mathbf{c}]_k$ if $j = k \in X_\lambda$ and is zero otherwise, preserves the nestling order components, but zeros out fledged orders. Thus $I_\Lambda - \Pi_{X_\lambda}^{\mathrm{T}}\Pi_{X_\lambda}$ keeps the fledged order components, and zeros the nestlings. Similarly, $\left[\Pi_{G_\lambda}^{\mathrm{T}}\Pi_{G_\lambda}\boldsymbol{\phi}\right]_{jk} = [\boldsymbol{\phi}]_k$ if $j = k \in G_\lambda$ and is zero otherwise. A little thought shows the fledged system has

$$\mathbf{Q}_\lambda = \Pi_{G_\lambda}\mathbf{Q}_\Lambda\Pi_{X_\lambda}^{\mathrm{T}}. \tag{13}$$

Standard Fourier example: Take $\Lambda = 2$, then for $\lambda = 1$; the standard Fourier example has

$$\Pi_{X_1} = \begin{bmatrix} 1 & 0 & 0 & 0 \\ 0 & 1 & 0 & 0 \end{bmatrix} \text{ and } \Pi_{G_1} = \begin{bmatrix} 1 & 0 & 0 & 0 \\ 0 & 0 & 1 & 0 \end{bmatrix}.$$

Scattering Fourier example: For the same levels, the scattering case has

$$\Pi_{X_1} = \begin{bmatrix} 0 & 1 & 0 & 0 \\ 0 & 0 & 0 & 1 \end{bmatrix} \text{ and } \Pi_{G_1} = \begin{bmatrix} 1 & 0 & 0 & 0 \\ 0 & 1 & 0 & 0 \end{bmatrix}. \tag{14}$$

3.5.2 Telescoping Difference Operators

One can now extend $\mathbf{R}_\lambda$ and $\mathbf{Q}_\lambda$ to common ranges and domains. Denote $Q_\lambda : C_\Lambda \to \Phi_\Lambda$ and $R_\lambda : \Phi_\Lambda \to C_\Lambda$ by

$$Q_\lambda = \Pi_{G_\lambda}^{\mathrm{T}}\mathbf{Q}_\lambda\Pi_{X_\lambda} \text{ and } R_\lambda = \Pi_{X_\lambda}^{\mathrm{T}}\mathbf{R}_\lambda\Pi_{G_\lambda} \tag{15}$$

then one may correctly write

$$\Delta_\lambda = R_\lambda - R_{\lambda-1},\ \lambda > 0$$
$$\Delta_0 = R_0. \tag{16}$$

Computationally, $\mathbf{R}_{\lambda-1}$ is simply subtracted from the components of $\mathbf{R}_\lambda$ determined by $G_{\lambda-1}$ and $X_{\lambda-1}$. The obvious telescoping result is

$$R_\lambda = \sum_{\kappa\le\lambda}\Delta_\kappa. \tag{17}$$

Scattering Fourier example: The maximum level $\Lambda = 2$, $N_\Lambda = 4$, then for level 1

$$Q_1 = \frac{1}{2}\begin{bmatrix} 0 & 1 & 0 & 1 \\ 0 & -i & 0 & i \\ 0 & 0 & 0 & 0 \\ 0 & 0 & 0 & 0 \end{bmatrix} \text{ and } R_1 = \begin{bmatrix} 0 & 0 & 0 & 0 \\ 1 & i & 0 & 0 \\ 0 & 0 & 0 & 0 \\ 1 & -i & 0 & 0 \end{bmatrix}.$$

The combination of telescoping and projection means that the Δ_λ coefficients computed at higher levels do not change lower-level order results. Interpreted in operator form, this gives the technical key to the Smolyak functional recovery in tensor spaces:

Projection Lemma: If $\kappa < \lambda$ then

$$\Delta_\lambda Q_\Lambda\Pi_{X_\kappa}^{\mathrm{T}} = 0. \tag{18}$$

Proof: This only applies to differences in $\Delta_\lambda Q_\Lambda\Pi_{X_\kappa}^{\mathrm{T}} = (R_\lambda - R_{\lambda-1})\,Q_\Lambda\Pi_{X_\kappa}^{\mathrm{T}} = T_1 - T_2$. The rest of the proof looks like an associative shell game on projections: After distribution, the first term has $T_1 = R_\lambda Q_\Lambda\Pi_{X_\kappa}^{\mathrm{T}} = \Pi_{X_\lambda}^{\mathrm{T}}\mathbf{R}_\lambda\Pi_{G_\lambda}Q_\Lambda\Pi_{X_\kappa}^{\mathrm{T}} = \Pi_{X_\lambda}^{\mathrm{T}}\mathbf{R}_\lambda\Pi_{G_\lambda}Q_\Lambda\left(\Pi_{X_\lambda}^{\mathrm{T}}\Pi_{X_\lambda}\right)\Pi_{X_\kappa}^{\mathrm{T}}$, the last insertion is permitted by the nesting $X_\kappa \subset X_\lambda$. Equation (13) means $T_1 = \Pi_{X_\lambda}^{\mathrm{T}}\mathbf{R}_\lambda\mathbf{Q}_\lambda\Pi_{X_\lambda}\Pi_{X_\kappa}^{\mathrm{T}} = \Pi_{X_\lambda}^{\mathrm{T}}I_{N_\lambda}\Pi_{X_\lambda}\Pi_{X_\kappa}^{\mathrm{T}} = \Pi_{X_\lambda}^{\mathrm{T}}\Pi_{X_\lambda}\Pi_{X_\kappa}^{\mathrm{T}} = \Pi_{X_\kappa}^{\mathrm{T}}$, again by nesting. The second term $T_2 = R_{\lambda-1}Q_\Lambda\Pi_{X_\kappa}^{\mathrm{T}} = \Pi_{X_\kappa}^{\mathrm{T}}$ by exactly the analogous computation for $\lambda - 1$. Thus $T_1 = T_2$ giving difference zero.

Scattering Fourier example: Maximum level $\Lambda = 2$, $N_\Lambda = 4$, then for level 1

$$\Delta_2 = \frac{1}{2}\begin{bmatrix} 1 & -1 & 1 & -1 \\ -1 & -i & -1 & -i \\ 1 & 1 & 1 & 1 \\ -1 & i & -1 & i \end{bmatrix} \text{ and } \Delta_2 Q_2 \Pi_{X_1}^{\mathrm{T}} = \frac{1}{2}\Delta_2 \begin{bmatrix} 1 & 1 \\ -i & i \\ -1 & -1 \\ i & -i \end{bmatrix} = \begin{bmatrix} 0 & 0 \\ 0 & 0 \\ 0 & 0 \\ 0 & 0 \end{bmatrix}.$$

4. MULTIDIMENSIONAL SMOLYAK GRIDDING AND ORDER

4.1 Multidimensional Tensor Products

The main thrust of this section will be to show tensor products of EDOs are again tensor EDOs, then to review the telescoping sums and the projection lemma in higher dimensions. This involves turning cranks, starting with the handles.

4.1.1 Definitions

Start with continuous systems $\left(I^d,\, X^d_{\lambda_d},\, \mathbb{O}^d_{\lambda_d},\, \mu^d\right)$ in dimensions $1 \le d \le D$. The distribution of independent random parameters $\Xi^d \in I^d$, $d = 1, \ldots, D$ each have PDF μ_d, and corresponding orthonormal polynomials $P^k_d,\, P^l_d \in \mathbb{O}^d_{\lambda_d}$, $k, l \in X^d$ with respect to inner product $\left(P^k_d,\, P^l_d\right)_j = \int P^k_d P^l_d \mu_j = \delta_{kl}$. A set of orders is the set of multi-indices $X_{\boldsymbol{\lambda}} = X^1_{\lambda_1} \times \cdots \times X^D_{\lambda_D}$ and the set of all orders is $X_{\boldsymbol{\Lambda}} = X^1_\Lambda \times \cdots \times X^D_\Lambda$, where each dimension has the same maximal level Λ. By independence, the multidimensional polynomials are simply products of the single variable ones. Thus, $P^{\mathbf{j}} = P_1^{j_1} \cdots P_D^{j_D}$ where the multi-index $\mathbf{j} = (j_1, \ldots, j_D) \in X_{\boldsymbol{\lambda}}$, and one may write $\mathbb{O}_{\boldsymbol{\lambda}} = \left\{P^{\mathbf{j}} : \mathbf{j} \in X_{\boldsymbol{\lambda}}\right\}$. Define $|\mathbf{j}| = \sum_{d=1}^D j_d$; inequalities $\mathbf{j} \le \mathbf{k}$, $\mathbf{j} < N$, and so forth, hold if the inequality holds componentwise. For $\boldsymbol{\xi} = (\xi_1, \ldots, \xi_D) \in I^{\mathbf{D}} = I^1 \times \cdots \times I^D$, the function $f(\boldsymbol{\xi}) \in \mathcal{L}(\mathbb{O}_{\boldsymbol{\lambda}})$ can be expanded in terms of the multidimensional FPC expansions of the form

$$f = \sum_{\mathbf{j} \in X_{\boldsymbol{\lambda}}} c_{\mathbf{j}} P^{\mathbf{j}}. \tag{19}$$

Note that $X_{\boldsymbol{\lambda}}$ indexes the product spaces of coefficients $C_{\boldsymbol{\lambda}} = C^1_\lambda \times \cdots \times C^D_{\lambda_D}$, so that $c_{\mathbf{j}} = [\mathbf{c}]_{\mathbf{j}}$ if $\mathbf{c} \in C_{\boldsymbol{\lambda}}$ and $\mathbf{j} \in X_{\boldsymbol{\lambda}}$. If the FPC expansions for $\boldsymbol{\lambda} = \boldsymbol{\Lambda}$ are uniformly of the same order $N_\Lambda = N\left(X^d_\Lambda\right)$, over the complete set of indices $X_{\boldsymbol{\Lambda}} c$ the sum in (19) has N_Λ terms in each dimension, giving $(N_\Lambda)^D$ terms. The coefficient is found by the inner product

$$c_{\mathbf{j}} = \left(P^{\mathbf{j}},\, f\right) = \int_{I^{\mathbf{D}}} \bar{P}^{\mathbf{j}} f\, \mu^{\mathbf{D}} d\xi_{\mathbf{D}} \tag{20}$$

with $\mu^{\mathbf{D}} = \mu_1 \cdots \mu_D$ and $d\xi_{\mathbf{D}} = d\xi_1 \ldots d\xi_D$. This completes the definition of the continuous orthonormal system $\left(I^{\mathbf{D}},\, X_{\boldsymbol{\lambda}},\, \mathbb{O}_{\boldsymbol{\lambda}},\, \mu^{\mathbf{D}}\right)$.

For the discretized system the maximal computational grid is the grid indices $\Xi_{\boldsymbol{\Lambda}} = \Xi^1_\Lambda \times \cdots \times \Xi^D_\Lambda$ and sub-grids can be selected from this by the multi-indices $G_{\boldsymbol{\lambda}} = G^1_{\lambda_1} \times \cdots \times G^D_{\lambda_D}$. Define the product weight set $W_{\boldsymbol{\lambda}} = \left\{w_{\mathbf{m}} = w^1_{m_1} \cdots w^D_{m_D} : \mathbf{m} \in G_{\boldsymbol{\lambda}}\right\}$ as the product of weights. The tensor production operator $\mathbf{Q}_{\boldsymbol{\lambda}} = \mathbf{Q}_{\lambda_1} \otimes \cdots \otimes \mathbf{Q}_{\lambda_D}$ can be constructed from the corresponding coefficients of the tensor matrix product so that its components are products

$$[\mathbf{Q}_{\boldsymbol{\lambda}}]_{\mathbf{jk}} = [\mathbf{Q}_{\lambda_1}]_{j_1 k_1} \cdots [\mathbf{Q}_{\lambda_D}]_{j_D k_D} = w_{j_1} P^{k_1}\left(\xi^{j_1}\right) \cdots w_{j_D} P^{k_D}\left(\xi^{j_D}\right) = w_{\mathbf{j}} P^{\mathbf{k}}\left(\xi^{\mathbf{j}}\right) \tag{21}$$

where $\xi^{\mathbf{j}} = \left(\xi_1^{j_1}, \ldots, \xi_D^{j_D}\right)$, $\mathbf{j} \in G_{\boldsymbol{\lambda}}$, $\mathbf{k} \in X_{\boldsymbol{\lambda}}$ and maps from the equivalent product spaces of coefficient vectors $C_{\boldsymbol{\lambda}} = C^1_\Lambda \times \cdots \times C^D_\Lambda$ to the product space of weighted evaluation at grid points $\Phi_{\boldsymbol{\lambda}} = \Phi^1_{\lambda_1} \times \cdots \times \Phi^D_{\lambda_D}$ by

$$[\mathbf{Q}_{\boldsymbol{\lambda}} \mathbf{c}_{\boldsymbol{\lambda}}]_{\mathbf{j}} = [\mathbf{Q}_{\lambda_1} \mathbf{c}_{\lambda_1}]_{j_1} \cdots [\mathbf{Q}_{\lambda_D} \mathbf{c}_{\lambda_D}]_{j_D} \text{ and } [\mathbf{R}_{\boldsymbol{\lambda}} \boldsymbol{\phi}_{\boldsymbol{\lambda}}]_{\mathbf{k}} = \left[\mathbf{R}_{\lambda_1} \boldsymbol{\phi}_{\lambda_1}\right]_{k_1} \cdots \left[\mathbf{R}_{\lambda_D} \boldsymbol{\phi}_{\lambda_D}\right]_{k_D}. \tag{22}$$

Set $\Pi_{G_{\boldsymbol{\lambda}}} = \Pi^1_{G_1} \otimes \cdots \otimes \Pi^D_{G_D}$, $\Pi^{\mathrm{T}}_{X_{\boldsymbol{\lambda}}} = \left(\Pi^1_{X_1}\right)^{\mathrm{T}} \otimes \cdots \otimes \left(\Pi^D_{X_D}\right)^{\mathrm{T}}$, and so forth. Note that $\Pi_{X_{\boldsymbol{\lambda}}} \Pi^{\mathrm{T}}_{X_{\boldsymbol{\lambda}}} = I_{X_{\boldsymbol{\lambda}}}$, the identity on $C_{\boldsymbol{\lambda}}$, for example. Also $\mathbf{Q}_{\boldsymbol{\lambda}} = \Pi_{G_{\boldsymbol{\lambda}}} Q_{\boldsymbol{\Lambda}} \Pi^{\mathrm{T}}_{X_{\boldsymbol{\lambda}}} = \mathbf{Q}^1_{\lambda_1} \otimes \cdots \otimes \mathbf{Q}^D_{\lambda_D}$ and $Q_{\boldsymbol{\lambda}} = \Pi^{\mathrm{T}}_{G_{\boldsymbol{\lambda}}} \mathbf{Q}_{\boldsymbol{\lambda}} \Pi_{X_{\boldsymbol{\lambda}}}$. Similarly for $\mathbf{R}_{\boldsymbol{\lambda}} = \mathbf{R}^1_{\lambda_1} \otimes \cdots \otimes \mathbf{R}^D_{\lambda_D}$ and $R_{\boldsymbol{\lambda}} = \Pi^{\mathrm{T}}_{X_{\boldsymbol{\lambda}}} \mathbf{R}_{\boldsymbol{\lambda}} \Pi_{G_{\boldsymbol{\lambda}}}$. This defines the discrete system $(G_{\boldsymbol{\lambda}},\, X_{\boldsymbol{\lambda}},\, \mathbf{R}_{\boldsymbol{\lambda}},\, W_{\boldsymbol{\lambda}})$.

4.1.2 Tensor EDO Systems

Next turn to showing $(G_{\boldsymbol{\lambda}},\, X_{\boldsymbol{\lambda}},\, \mathbf{R}_{\boldsymbol{\lambda}},\, W_{\boldsymbol{\lambda}})$ is an EDO of $\left(I^{\mathbf{D}},\, X_{\boldsymbol{\lambda}},\, \mathbb{O}_{\boldsymbol{\lambda}},\, \mu^{\mathbf{D}}\right)$ and, in particular,

EDO theorem (tensor products): $\left(I^{\mathbf{D}},\, X_{\boldsymbol{\lambda}},\, \mathbb{O}_{\boldsymbol{\lambda}},\, \mu^{\mathbf{D}}\right)$ is an EDO system with discretization $(G_{\boldsymbol{\lambda}},\, X_{\boldsymbol{\lambda}},\, \mathbf{R}_{\boldsymbol{\lambda}},\, W_{\boldsymbol{\lambda}})$ if and only if

$$\mathbf{R}_{\boldsymbol{\lambda}} = \mathbf{Q}_{\boldsymbol{\lambda}}^{-1}, \text{ where } \left[\mathbf{Q}_{\boldsymbol{\lambda}}\right]_{\mathbf{jk}} = (w_{\mathbf{k}})\, P^{\mathbf{j}}\left(\xi^{\mathbf{k}}\right),\ \mathbf{j} \in X_{\boldsymbol{\lambda}} \text{ and } \mathbf{k} \in G_{\boldsymbol{\lambda}}. \tag{23}$$

Proof: It suffices to re-express (23) via its single dimension constituents. For the integral, begin by separating each dimension

$$c_{\mathbf{j}} = \int_{I^{\mathbf{D}}} \bar{P}^{\mathbf{j}} f\, \mu_{\mathbf{D}} d\xi_{\mathbf{D}} = \int_{I^1} \bar{P}^{j_1} \mu_1 d\xi_1 \cdots \int_{I^D} \bar{P}^{j_D} \mu_D d\xi_D f\left(\xi_1, \ldots, \xi_D\right).$$

By the EDO property in each dimension, each of these becomes a sum

$$c_{\mathbf{j}} = \sum_{m_1 \in G_{\lambda_1}} \left[\mathbf{R}_{\lambda_1}\right]_{j_1 m_1} w_{,m_1} \cdots \sum_{m_D \in G_{\lambda_D}} \left[\mathbf{R}_{\lambda_D}\right]_{j_D m_D} w_{,m_D} f\left(\xi^{m_1}, \ldots, \xi^{m_D}\right).$$

Group terms for $\mathbf{R}_{\boldsymbol{\lambda}}$ and $w_{\mathbf{m}}$

$$c_{\mathbf{j}} = \sum_{\mathbf{m} \in G_{\boldsymbol{\lambda}}} \left[\mathbf{R}_{\boldsymbol{\lambda}}\right]_{\mathbf{jm}} w_{\mathbf{m}} f\left(\xi^{\mathbf{m}}\right) = \left[\mathbf{R}_{\boldsymbol{\lambda}} \boldsymbol{\phi}_{\boldsymbol{\lambda}}\right]_{\mathbf{j}}, \tag{24}$$

where $\left[\boldsymbol{\phi}_{\boldsymbol{\lambda}}\right]_{\mathbf{m}} = w_{\mathbf{m}} f\left(\xi^{\mathbf{m}}\right)$, with the vector grid point $\xi^{\mathbf{m}} = \left(\xi^{m_1}, \ldots, \xi^{m_D}\right) \in \Xi_{\boldsymbol{\lambda}}$. Thus there is a matrix multiplication (albeit multi-indexed) that is equivalent to the integral, and so it is an EDO by definition. Using $\mathbf{R}_{\lambda_d} = \mathbf{Q}_{\lambda_d}^{-1}$ and assembling into a tensor for $\mathbf{j}, \mathbf{k} \in X_{\boldsymbol{\lambda}}$, $\left[\mathbf{R}_{x_{\boldsymbol{\lambda}}}\right]_{\mathbf{jk}} = \left[\mathbf{R}_{\lambda_1} \otimes \cdots \otimes \mathbf{R}_{\lambda_D}\right]_{\mathbf{jk}} = \left[\mathbf{Q}_{\lambda_1}^{-1}\right]_{j_1 k_1} \cdots \left[\mathbf{Q}_{\lambda_D}^{-1}\right]_{j_D k_D} = \left[\mathbf{Q}_{\boldsymbol{\lambda}}^{-1}\right]_{\mathbf{jk}}$, or $\mathbf{R}_{\boldsymbol{\lambda}} = \mathbf{Q}_{\boldsymbol{\lambda}}^{-1}$. Concretely for $\mathbf{k} \in G_{\boldsymbol{\lambda}}$, componentwise for $\mathbf{c} \in C_{\boldsymbol{\lambda}}$

$$\phi_{\mathbf{k}} = \left[Q_{\boldsymbol{\lambda}} \mathbf{c}\right]_{\mathbf{k}} = w_{\mathbf{k}} \sum_{\mathbf{j} \in X_{\boldsymbol{\lambda}}} c_{\mathbf{j}} P^{\mathbf{j}}\left(\xi^{\mathbf{k}}\right) = \sum_{\mathbf{j} \in X_{\boldsymbol{\lambda}}} c_{\mathbf{j}} \left[w_{k_1}^1 P_1^{j_1}\left(\xi_1^{k_1}\right) \cdots w_{k_1}^1 P_D^{j_D}\left(\xi_D^{k_D}\right)\right], \tag{25}$$

where $c_{\mathbf{j}} = \left[\mathbf{c}\right]_{\mathbf{j}}$. This gives the final term of (23).

Because the tensor system is built from single dimensional ones, existence of fledged systems derives from those criterion this gives a instead of existence.

EDO fledging lemma (tensor products): Suppose $\left(G_\lambda^d,\, X_\lambda^d,\, \mathbf{R}_\lambda^d,\, W_\lambda^d\right)$ are EDO systems, $1 \le d \le D$, $0 \le \lambda \le \Lambda$. Additionally $0 \le \boldsymbol{\kappa} \le \boldsymbol{\lambda} \le \Lambda$ (componentwise) and for some d $\kappa^d < \lambda^d$. Then $(G_{\boldsymbol{\kappa}},\, X_{\boldsymbol{\kappa}},\, \mathbf{R}_{\boldsymbol{\kappa}},\, W_{\boldsymbol{\kappa}}) \lessdot (G_{\boldsymbol{\lambda}},\, X_{\boldsymbol{\lambda}},\, \mathbf{R}_{\boldsymbol{\lambda}},\, W_{\boldsymbol{\lambda}})$ and $\mathbf{Q}_{\boldsymbol{\kappa}} = \Pi_{G_{\boldsymbol{\kappa}}} Q_{\boldsymbol{\lambda}} \Pi_{X_{\boldsymbol{\kappa}}}^{\mathrm{T}}$.

Proof: Product space rules give $X_{\boldsymbol{\kappa}} \subset X_{\boldsymbol{\lambda}}$ and $G_{\boldsymbol{\kappa}} \subset G_{\boldsymbol{\lambda}}$. Because of the latter the indices of the weights are nested so $W_{\boldsymbol{\kappa}} \subset W_{\boldsymbol{\lambda}}$. For individual dimensions $\mathbf{Q}_{\kappa_d} = \Pi_{G_{\kappa_d}} Q_{\lambda_d} \Pi_{X_{\kappa_d}}^{\mathrm{T}}$. Then assembly of tensors gives tensor identity.

4.1.3 Telescoping and Projection Lemma

Finally, define the tensor difference maps

$$\Delta_{\boldsymbol{\lambda}} = \Delta_{\lambda_1} \otimes \cdots \otimes \Delta_{\lambda_D}. \tag{26}$$

Induction on dimension (see Wasilkowski and Woźniakowski [23]) shows the tensor telescoping term

$$R_{\boldsymbol{\lambda}} = \sum_{\boldsymbol{\kappa} \le \boldsymbol{\lambda}} \Delta_{\boldsymbol{\kappa}}. \tag{27}$$

Tensor Projection Lemma: If for some $1 \le d \le D$, $\kappa_d < \lambda_d$ then

$$\Delta_{\boldsymbol{\lambda}} Q_{\boldsymbol{\Lambda}} \Pi_{X_{\boldsymbol{\kappa}}}^{\mathrm{T}} = 0. \tag{28}$$

Proof: For $\kappa_d < \lambda_d$, $\Delta_{\lambda_d} Q_\Lambda^d \Pi_{X_{\kappa_d}}^{\mathrm{T}} = 0$, so $\Delta_{\boldsymbol{\lambda}} Q_{\boldsymbol{\Lambda}} \Pi_{X_{\boldsymbol{\kappa}}}^{\mathrm{T}} = \left(\Delta_{\lambda_1} Q_\Lambda^1 \Pi_{X_{\kappa_1}}^{\mathrm{T}}\right) \otimes \cdots \otimes (0) \otimes \cdots \otimes \left(\Delta_{\lambda_D} Q_\Lambda^D \Pi_{X_{\kappa_D}}^{\mathrm{T}}\right) = 0$ by the Projection Lemma (18).

All the pieces are now here for the Smolyak construction.

5. SMOLYAK CONSTRUCTION

The Smolyak construction includes sums over levels tensor product. First define the Smolyak sparse grid set and its index set

$$\Xi_S = \bigcup_{|\boldsymbol{\lambda}|=\Lambda} \Xi_{\boldsymbol{\lambda}} = \bigcup_{|\boldsymbol{\lambda}|\leq\Lambda} \Xi_{\boldsymbol{\lambda}} \text{ and } G_S = \bigcup_{|\boldsymbol{\lambda}|=\Lambda} G_{\boldsymbol{\lambda}} = \bigcup_{|\boldsymbol{\lambda}|\leq\Lambda} G_{\boldsymbol{\lambda}} \tag{29}$$

as well as the set of orthonormal functions and their sparse Smolyak order index set

$$\mathbb{O}_S = \bigcup_{|\boldsymbol{\lambda}|=\Lambda} \mathbb{O}_{\boldsymbol{\lambda}} = \bigcup_{|\boldsymbol{\lambda}|\leq\Lambda} \mathbb{O}_{\boldsymbol{\lambda}}. \text{ and } X_S = \bigcup_{|\boldsymbol{\lambda}|=\Lambda} X_{\boldsymbol{\lambda}} = \bigcup_{|\boldsymbol{\lambda}|\leq\Lambda} X_{\boldsymbol{\lambda}}. \tag{30}$$

The set $\mathcal{L}(\mathbb{O}_S)$ contains polynomials of the form

$$f = \sum_{\mathbf{j}\in X_S} c_{\mathbf{j}} P^{\mathbf{j}}. \tag{31}$$

The set of weighted functional evaluations, Φ_S, consists of vectors $\mathcal{E}_S f$ with components given by $\xi^{\mathbf{k}} \in \Xi_S$, $\mathbf{k} \in G_S$

$$[\mathcal{E}_S f]_{\mathbf{k}} = w_{\mathbf{k}} f\left(\xi^{\mathbf{k}}\right) = \sum_{\mathbf{j}\in X_S} c_{\mathbf{j}} w_{\mathbf{k}} P^{\mathbf{j}}\left(\xi^{\mathbf{k}}\right) = \sum_{\mathbf{j}\in X_S} c_{\mathbf{j}} \left[\mathbf{Q}_S\right]_{\mathbf{kj}} \tag{32}$$

where $c_{\mathbf{j}} = [\mathbf{c}]_{\mathbf{j}}$, $\mathbf{c} \in C_S = \{\mathbf{c} : \mathbf{c}_{\mathbf{j}} \in C_{\boldsymbol{\Lambda}}, \mathbf{j} \in X_S\}$. The final part of (32) defines $\mathbf{Q}_S$ componentwise. The projection operators $\Pi_{X_S} : C_{\boldsymbol{\Lambda}} \to C_S$ and $\Pi_{G_S} : \Phi_{\boldsymbol{\Lambda}} \to \Phi_S$ track non-zero indices algebraically within the complete product space of indices. Numerically, standard computational techniques handle the sparsity of Π_{X_S} and Π_{G_S}, as well as of the Smolyak computations generallly. The projections appear here formally, and also help define $\mathbf{Q}_S = \Pi_{G_S} Q_{\boldsymbol{\Lambda}} \Pi_{X_S}^{\mathrm{T}}$. Theoretically $\mathbf{R}_S = \mathbf{Q}_S^{-1}$ could apply computationally, but the following lower-cost method works:

Smolyak construction for EDO: The Smolyak system $(G_S,\, X_S,\, \mathbb{O}_S,\, W_S)$ has EDO $(G_S,\, X_S,\, \mathbf{R}_S,\, W_S)$ with

$$R_S = \sum_{|\boldsymbol{\lambda}|\leq\Lambda} \Delta_{\boldsymbol{\lambda}} \tag{33}$$

which defines $\mathbf{R}_S = \Pi_{X_S} R_S \Pi_{G_S}^{\mathrm{T}}$. Then

$$\mathbf{R}_S = \mathbf{Q}_S^{-1} \tag{34}$$

and $\mathbf{R}_S$ will be called the *Smolyak matrix*.

Proof: By the linearity, it suffices to demonstrate that $\mathbf{R}_S\mathbf{Q}_S$ is the identity on C_S for each component. Select any component index $\mathbf{j} \in X_S$, and then find the smallest level index $\boldsymbol{\kappa}$ with $\mathbf{j} \in X_{\boldsymbol{\kappa}} \subset X_S$. Because the of the projection theorem, the contributions from order index $\mathbf{j}$ occur in levels up to $\boldsymbol{\kappa}$. Thus, for convenience, introduce vector $\boldsymbol{\delta}_{\mathbf{j}} \in C_{\boldsymbol{\kappa}}$ with $[\boldsymbol{\delta}_{\mathbf{j}}]_{\mathbf{m}} = 1$ if $\mathbf{m} = \mathbf{j}$ and is zero otherwise. This will zero pad to higher levels as needed. Such $\boldsymbol{\delta}_{\mathbf{j}}$ corresponds to $\boldsymbol{\phi} \in \Phi_S$ with $\phi_{\mathbf{k}} = [\boldsymbol{\phi}]_{\mathbf{k}} = \left[\mathcal{E}_S P^{\mathbf{j}}\right]_{\mathbf{k}} = w_{\mathbf{k}} P^{\mathbf{j}}\left(\xi^{\mathbf{k}}\right) = [\mathbf{Q}_S]_{\mathbf{kj}}$. Then $\phi_{\mathbf{k}} = \left[\mathbf{Q}_S \Pi_{X_S} \Pi_{X_\kappa}^{\mathrm{T}}\right]_{\mathbf{kj}} = \left[\Pi_{G_S} Q_S \Pi_{X_\kappa}^{\mathrm{T}}\right]_{\mathbf{kj}}$ since Π_{X_κ} projects to $C_{\boldsymbol{\kappa}}$ which contains vectors with the correct index $\mathbf{j}$. For $\boldsymbol{\delta}_{\mathbf{j}}$, $\phi_{\mathbf{k}} = \left[\Pi_{G_S} Q_S \Pi_{X_\kappa}^{\mathrm{T}} \boldsymbol{\delta}_{\mathbf{j}}\right]_{\mathbf{k}}$. Zero pad $\boldsymbol{\phi}$ to all indices with $\tilde{\boldsymbol{\phi}} = \Pi_{G_S}^{\mathrm{T}} \boldsymbol{\phi} = \Pi_{G_S}^{\mathrm{T}} \Pi_{G_S} Q_S \Pi_{X_\kappa}^{\mathrm{T}} \boldsymbol{\delta}_{\mathbf{j}} = Q_S \Pi_{X_\kappa}^{\mathrm{T}} \boldsymbol{\delta}_{\mathbf{j}}$ since projections have exactly the same non-zero structure as Q_S. One needs to show $R_S \tilde{\boldsymbol{\phi}} = \tilde{\boldsymbol{\delta}}_{\mathbf{j}}$ where the extended $\tilde{\boldsymbol{\delta}}_{\mathbf{j}} \in C_{\boldsymbol{\Lambda}}$ has $\left[\tilde{\boldsymbol{\delta}}_{\mathbf{j}}\right]_{\mathbf{m}} = 1$ if $\mathbf{m} = \mathbf{j}$ and is zero otherwise. Substituting for $\tilde{\boldsymbol{\phi}}$ in (33) gives

$$R_S \tilde{\boldsymbol{\phi}} = \sum_{|\boldsymbol{\lambda}|\leq\Lambda} \Delta_{\boldsymbol{\lambda}} \tilde{\boldsymbol{\phi}} = \sum_{|\boldsymbol{\lambda}|\leq\Lambda} \Delta_{\boldsymbol{\lambda}} Q_S \Pi_{X_\kappa}^{\mathrm{T}} \boldsymbol{\delta}_{\mathbf{j}}. \tag{35}$$

Now separate (35) into two sums

$$\left\{R_S \tilde{\boldsymbol{\phi}}\right\}_{\mathrm{LE}} = \sum_{\boldsymbol{\lambda}\leq\boldsymbol{\kappa}} \Delta_{\boldsymbol{\lambda}} Q_S \Pi_{X_\kappa}^{\mathrm{T}} \boldsymbol{\delta}_{\mathbf{j}} \text{ and } \left\{R_S \tilde{\boldsymbol{\phi}}\right\}_{\mathrm{NLE}} = \sum_{\boldsymbol{\lambda}\not\leq\boldsymbol{\kappa}, |\boldsymbol{\lambda}|\leq\Lambda} \Delta_{\boldsymbol{\lambda}} Q_S \Pi_{X_\kappa}^{\mathrm{T}} \boldsymbol{\delta}_{\mathbf{j}}. \tag{36}$$

Then $R_{\boldsymbol{\kappa}} = \sum_{\boldsymbol{\lambda} \leq \boldsymbol{\kappa}} \Delta_{\boldsymbol{\lambda}}$, and $\left\{ R_S \tilde{\boldsymbol{\phi}} \right\}_{\text{LE}} = R_{\boldsymbol{\kappa}} Q_S \Pi_{X_{\boldsymbol{\kappa}}}^{\text{T}} \boldsymbol{\delta}_{\mathbf{j}} = \Pi_{X_{\boldsymbol{\kappa}}}^{\text{T}} \mathbf{R}_{\boldsymbol{\kappa}} \Pi_{G_{\boldsymbol{\kappa}}} Q_S \Pi_{X_{\boldsymbol{\kappa}}}^{\text{T}} \boldsymbol{\delta}_{\mathbf{j}} = \Pi_{X_{\boldsymbol{\kappa}}}^{\text{T}} \mathbf{R}_{\boldsymbol{\kappa}} \mathbf{Q}_{\boldsymbol{\kappa}} \boldsymbol{\delta}_{\mathbf{j}} = \Pi_{X_{\boldsymbol{\kappa}}}^{\text{T}} \boldsymbol{\delta}_{\mathbf{j}} = \tilde{\boldsymbol{\delta}}_{\mathbf{j}}$, as required for identity. Turning to $\left\{ R_S \tilde{\boldsymbol{\phi}} \right\}_{\text{NLE}}$, for each term $\boldsymbol{\lambda} \nleq \boldsymbol{\kappa}$, scrutiny componentwise means that there is some d such that $\lambda_d > \kappa_d$ and so by the tensor projection lemma, $\Delta_{\boldsymbol{\lambda}} Q_S \Pi_{X_{\boldsymbol{\kappa}}}^{\text{T}} = 0$. $\left\{ R_S \tilde{\boldsymbol{\phi}} \right\}_{\text{NLE}} = 0$ as required.

Corollary (Exact Reconstruction): The Smolyak construction that most closely corresponds to standard quadrature

$$A_S = R_S \mathcal{E}_S : \mathcal{L}\left(\mathbb{O}_S\right) \rightarrow C_S \tag{37}$$

gives coefficients $\mathbf{c} = A_S f$ that reconstruct $f \in \mathcal{L}\left(\mathbb{O}_S\right)$ exactly via (31).

The form (37) extends to function spaces well approximated by $\mathcal{L}\left(\mathbb{O}_S\right)$; see Novak and Ritter [15]. Error estimates for such an example will be done numerically and are deferred to that section. They also point out

$$R_S = \sum_{\Lambda - D + 1 \geq |\boldsymbol{\lambda}| \leq \Lambda} (-1)^{|\boldsymbol{\lambda}| - 1} \left(\begin{array}{c} D-1 \\ |\boldsymbol{\lambda}| - 1 \end{array} \right) R_{\boldsymbol{\lambda}} \tag{38}$$

based on Delvos [22] or Wasilkowski and Woźniakowski [23]. Note that the cardinality of the sparse basis $N_S = N\left(\mathbb{O}_S\right) = N\left(\Xi_S\right)$ is identical to the sparse sample size. Re-interpreted in compressed sensing terms: For a K-sparse Smolyak EDO system, $K = N_S$ and K samples suffice.

5.1 Fourier-Laguerre Example

Using the level indices for the Fourier scattering and Laguerre examples, one can piece together the two-dimensional Smolyak sample points. For two-dimensions and level 4, the order indices are plotted in Fig. 2(a) and the corresponding sampling grid in Fig. 2(b). The grouping of points is indicated in column 2 of Table 3. The levels are indicated in the first column, and the additional points required for the level in the two-dimensional problem appear in the second column. The third column shows the Smolyak matrix condition number for the "top-down" fledging, where lower-level grid point selection from the higher-level grid results from maximizing the condition number given the set of lower-level orders. For comparison the next indicates the "bottom-up" fledging condition numbers, which are generally larger. The corresponding orders and grid points to the system give the Smolyak matrix $\mathbf{R}_S$, with symmetric indexing of non-zero entries, with amplitudes indicated in Fig. 2(c). The matrix is sparse with 44% non-zero elements, and at higher-dimensions becomes sparser with 15%, 3.7%, and 0.64% for 4, 8, and 16 dimensions, respectively. Note that the Smolyak matrix inverse, the matrix of weighted evaluation of the orthonormal functions $\mathbf{Q}_S = \mathbf{R}_S^{-1}$, is a full matrix. Hence, the true inversion to find $\mathbf{R}_S$ costs more than the Smolyak construction. The remainder of Table 3 shows higher dimensional Smolyak matrix condition numbers for 4, 8, and 16 dimensions, as well as the number of sample points (equivalently, orders). Even at 16 dimensions, the condition number indicates numerical errors many orders of magnitude smaller than the approximation tolerance used here.

6. ERROR ANALYSIS IN THE ACOUSTIC SCATTERING PROBLEM

The error analysis for the FPC representation of scattering from a single surface Fourier component appears in Fig. 3. The estimated error for the full 16×16 Fourier-Laguerre decomposition is about 10^{-4} compared to the 32×32 computation for orders shown in Fig. 1. The following error analysis focuses on a hypothetical vertical array with $M = 141$ phones at 1 m spacing from 10 to 150 m depth. Let $F_{kl}^{\text{r}}\left(z_m\right)$ be the reference coefficient of the acoustic field of Fourier order k and Laguerre order l at a depth z_m over M phones. The discrepancy of the coefficient computattion according to Smolyak $F_{kl}^{S}\left(z_m\right)$ is described as the error computed on root-mean-square (RMS) of differences $\text{Err} = \sqrt{1/M \sum_{m=1}^{M} |F_{kl}^{S}(z_m) - F_{kl}^{\text{r}}(z_m)|^2}$. Use of the Smolyak construction to compute various levels gives discrepancy errors from the full grid in Fig. 3(a). The horizontal axis is the same coefficient number indicated in Fig. 2(a) and for level 3 numbers inside Fig. 1. The absolute errors drop perhaps a factor of $1/5 \sim 10^{-0.7}$ for each additional level. The top level approximates that of the full grid computation. Indeed, the results reach virtually the same tolerance, and the

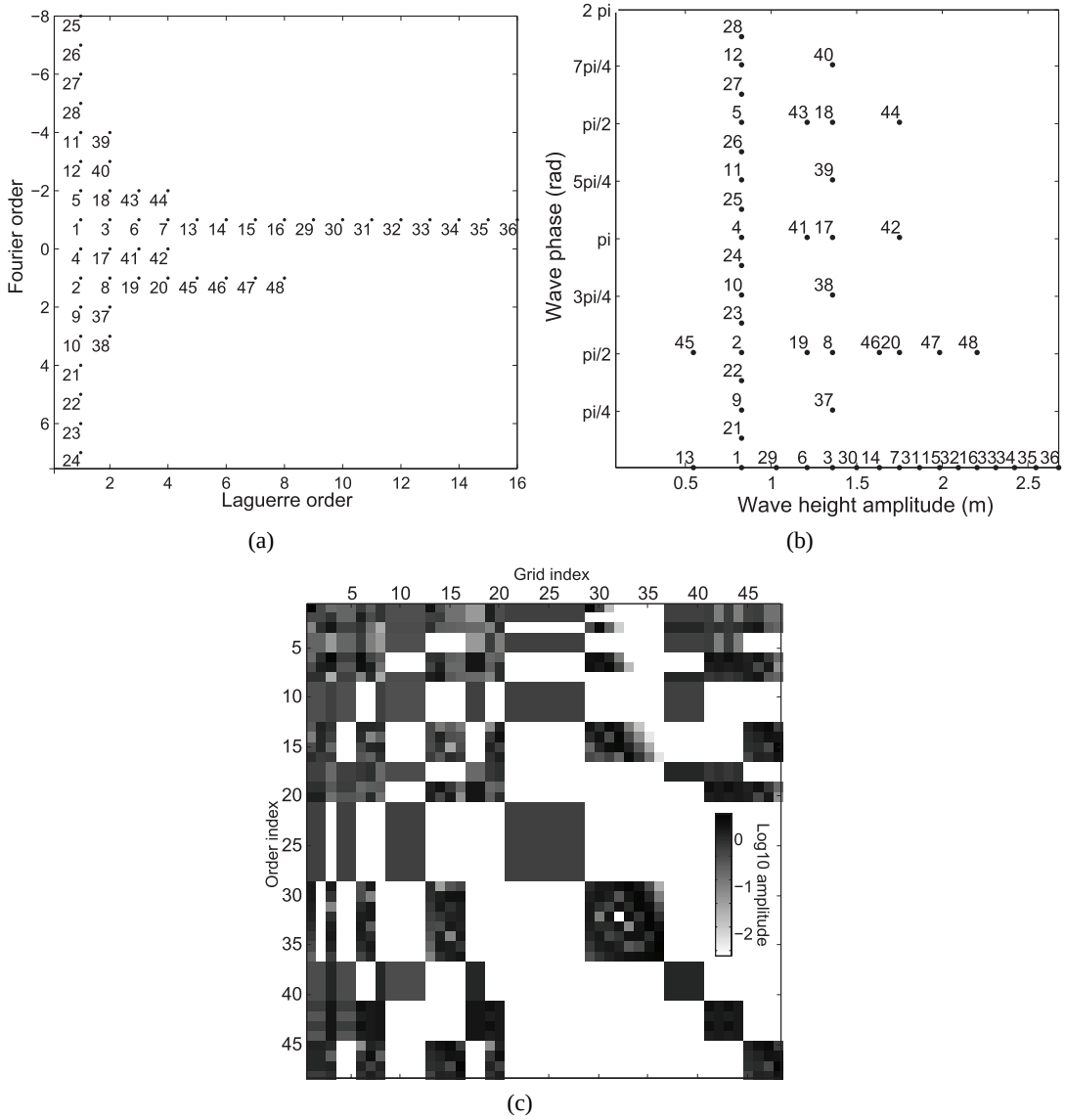

(a) (b)

(c)

FIG. 2: Fourier-Laguerre Smolyak construction orders (a) and grids (b) and the corresponding matrix (c).

TABLE 3: Number of points and condition number. 2-D top-down, bottom-up; $>$ 2-D, top-down only

	2-D			4-D,	d	8-D,	d	16-D,	d
Level	Added Pts	C#, d	C#, u	#Pt	C#	#Pt	C#	#Pt	C#
4	21-8, 29-36, 37-40, 41-4, 45-8	8.11	9.08	192	98.4	1059	1416	8021	51390
3	9-12, 13-6, 17-8, 19-20	5.99	6.65	63	35.2	253	338	1273	6982
2	4-5, 6-7, 8	3.95	3.51	19	11.0	53	68.8	169	719
1	2, 3	1.73	1.98	5	3.51	9	11.5	17	47.2
0	1	1							

Smolyak construction wins out based on 48 functional evaluations versus 256. The Fourier-Laguerre coefficients RMS $\text{Amp}^{\text{r}} = \sqrt{1/M \sum_{m=1}^{M} |F_{kl}^{\text{r}}(z_m)|^2}$ amplitudes vary from 10^{-5} to 1 along the horizontal axis in Fig. 3(b). The vertical

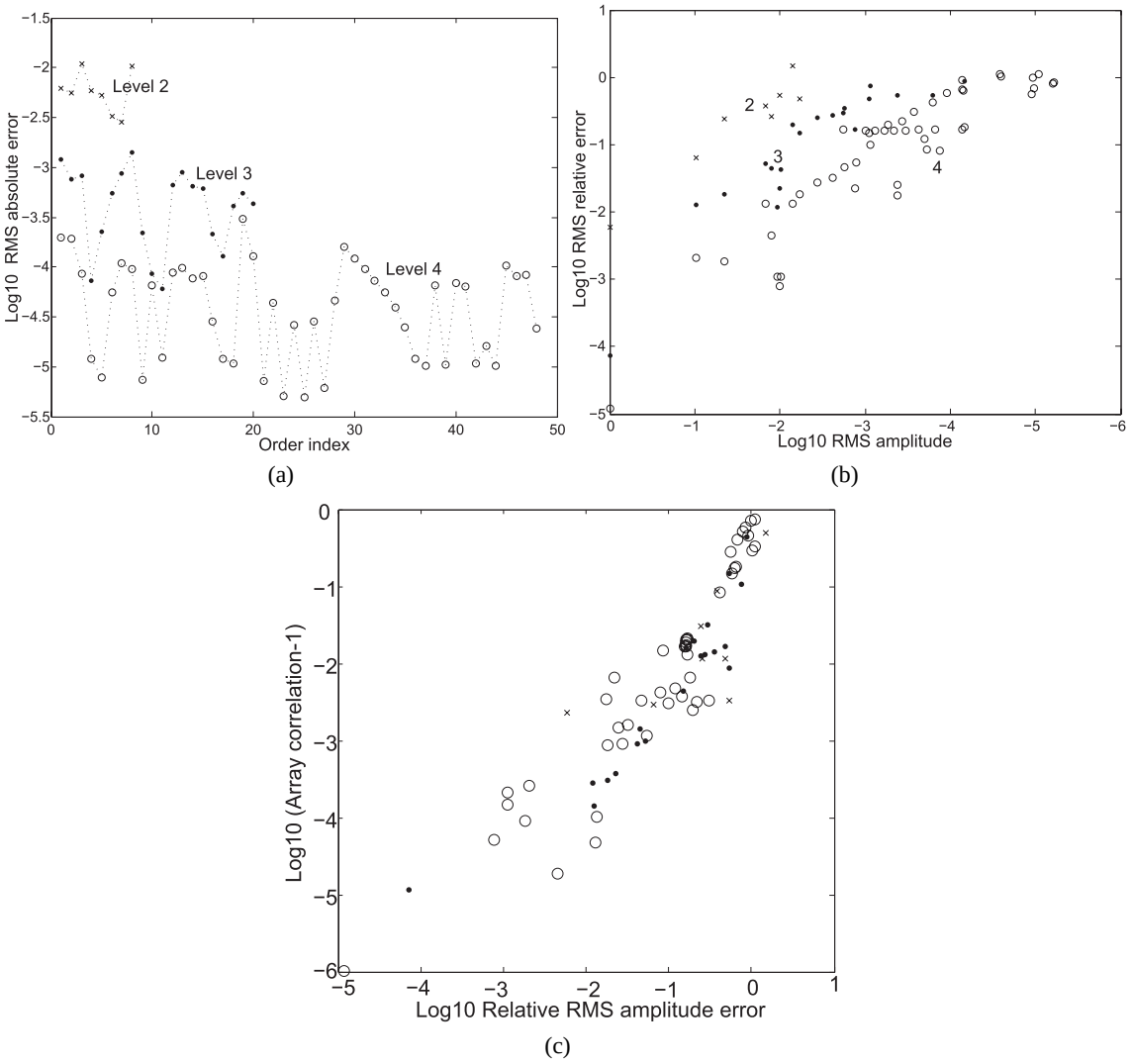

FIG. 3: Error analysis: absolute 3(a), relative 3(b), and phase correlation –1 along array 3(c). Levels: $2\times$, $3\cdot$, $4\circ$.

axis of relative error Re$l = \text{Err}/\text{Amp}^{\text{r}}$ varies almost inversely so as to maintain approximately the same absolute error. On the other hand, acoustic beam-forming requires an array. Beam-forming uses relative phase at phones along the array to determine direction of arrival. This permits separation of deeper angle reflections from the main reflection in the $(0,0)$ plot of Fig. 1 due to the variable surface height. Figure 3(c) addresses the error in phase by looking at the mean correlation along the array. If $F\left(z_k\right)$ is the acoustic field at a depth, the array averaged correlation is

$$\text{Corr} = \frac{\left| \dfrac{1}{M} \displaystyle\sum_{m=1}^{M} \bar{F}^{\text{r}}_{kl}\left(z_m\right) F^{S}_{kl}\left(z_m\right) \right|}{\text{Amp}^{\text{r}}\text{Amp}^{S}}.$$

This represents an amplitude weighted average of the phase difference. The result is normalized by the RMS amplitudes to give 1 if there is no discrepancy in the phase. Figure 3(c) plots the magnitude of the correlation difference from 1. The Smolyak construction coefficients have slightly better phase correlation than relative error, typically by

an order of magnitude. The statistics of beam-forming should have reliable phase components using the Smolyak method. Overall, the errors of the Smolyak construction compare favorably to the use of the full grid in this case.

7. CONCLUSIONS

The EDO criteria for study of PC and FPC Smolyak construction allow the study of minimal sampling: if a FPC expansion has orders compatible with a Smolyak construction, this paper outlines a recipe for picking the smallest number of samples that could recover such a representation. This idea represents an extension of Nyquist-Shannon sampling theory to multidimensional, sparse FPC representations. The new EDO criteria replace polynomial exactness and better express the idea of "multi-level PC exact" systems. This paper shows that Smolyak EDO systems actually achieve the minimal sample size for functional recovery. Additionally, the Smolyak matrix is sparse, further reducing computational loads.

By backing off from the typical idea of quadrature for PC or FPC coefficient calculations, and treating the problem algebraically, one can create nested sampling grids. In one dimension, the EDO criteria result in a fledged sub-matrix that produces the same PC coefficient values as the correct Gauss quadrature of the same abscissa count; this result bootstraps by tensor products to higher dimensions. The algebraic approach blurs the idea of the quadrature weights and polynomial exactness in favor of nested gridding and PC coefficient accuracy at specified orders. As noted, the weights included in the construction only relate to quadrature at the highest level. They allow the iterated fledging process in one dimension to create sufficient levels, each with sufficiently small condition number. When assembled into tensor products, the Smolyak EDO construction numerical accuracy can be quantified by condition numbers for worst case analysis. For the physical problem above, the approximation achieves the desired accuracy with a small fraction of the evaluation load over the use of a complete quadrature grid. In this study, the use of a sparse grid of level 3 fledged from level 4 abscissas and orders yields results well within tolerance compared to level 3 grid based on the "correct" level 3 abscissas and orders. This indicates that the penalty for lower-level computations using higher-level grid locations is quite low in this case. The method provides good estimates of mean phase variability and so is quite attractive to the acoustic scattering application.

The method here makes no use of specific level sizes or decimation rates. The construction requires only that tensor products of lower-dimension EDOs nest appropriately in higher-dimensional EDOs and that the nested systems follow the relatively weak conditions of Sections 4.1 and 5: meeting the criteria of the EDO theorem and the fledging and projection lemmas. Thus the method here should work for anisotropic cases, and varying order index truncation schemes similar to those outlined by Blatman in [24] and [25]. It should also extend to the multi-order 0 levels, fixed sample size across levels in some dimensions, and other idiosyncrasies.

The system of fledged EDOs and their assembly into multidimensional Smolyak EDOs represents a partially adaptive method of significant flexibility.

ACKNOWLEDGMENT

This research is sponsored by the Office of Naval Research.

REFERENCES

1. Baraniuk, R., Compressive sensing [lecture notes], *Signal Processing Magazine, IEEE*, 24(4):118–121, 2007.
2. Smolyak, S., Quadrature and interpolation formulas for tensor products of certain classes of functions, *Dokl. Akad. Nauk SSSR*, 4:240–243, 1963.
3. Ghanem, R. G. and Spanos, P. D., *Stochastic Finite Elements: A Spectral Approach*, rev. ed., Mineola, NY: Dover Publications, 2012.
4. Creamer, D. B., On using polynomial chaos for modeling uncertainty in acoustic propagation, *J. Acoust. Soc. Am.*, 119(4):1979–1994, 2006.
5. Finette, S., A stochastic representation of environmental uncertainty and its coupling to acoustic wave propagation in ocean waveguides, *J. Acoust. Soc. Am.*, 120(5):2567–2579, 2006.

6. Khine, Y. Y., Creamer, D. B., and Finette, S., Acoustic propagation in an uncertain waveguide environment using stochastic basis expansions, *J. Comput. Acoust.*, 18(4):397–441, 2010.
7. Hayward, T. J. and Oba, R. M., Convergence of polynomial chaos expansion based estimates of acoustic field and array beam response probability density functions, *J. Acoust. Soc. Am.*, 129(4):2601, 2011.
8. Gerstner, T. and Griebel, M., Numerical integration using sparse grids, *Num. Algorithms*, 18:209–232, 1998.
9. Patterson, T., The optimum addition of points to quadrature formulae, *Math. Comput.*, 22:847–856, 1968.
10. Laurie, D., Calculation of Gauss-Kronrod quadrature rules, *Math. Comput.*, 66:1133–1145, 1997.
11. Doostan, A. and Owhadi, H., A non-adapted sparse approximation of PDEs with stochastic inputs, *J. Comput. Phys.*, 230(8):3015–3034, 2011.
12. Novak, E. and Ritter, K., The curse of dimension and a universal method for numerical integration, In *Multivariate Approximation and Splines*, Basel: Birkhauser, pp. 177–187, 1998.
13. Temirgaliev, N., Kudaibergenov, S., and Shomanova, A., Applications of Smolyak quadrature formulas to the numerical integration of Fourier coefficients and in function recovery problems, *Russ. Math.*, 54(3):45–62, 2010.
14. Mathelin, L. and Gallivan, K., A compressed sensing approach for partial differential equations with random input data, *Commun. Comput. Phys.*, 12:919–954, 2012.
15. Novak, E. and Ritter, K., High dimensional integration of smooth functions over cubes, *Numer. Math.*, 75(1):79–97, 1996.
16. Szegö, G., *Orthogonal Polynomials*, number v. XXIII, American Mathematical Society, 1939.
17. Oba, R. M., Global boundary flattening transforms for acoustic propagation under rough sea surfaces, *J. Acoust. Soc. Am.*, 128(1):39–49, 2010.
18. Thorsos, E. I., The validity of the Kirchhoff approximation for rough surface scattering using a gaussian roughness spectrum, *J. Acoust. Soc. Am.*, 83(1):78–92, 1988.
19. Xiu, D. and Shen, J., An efficient spectral method for acoustic scattering from rough surfaces, *Commun. Comput. Phys.*, 2:54–72, 2007.
20. Golub, G. H. and Welsch, J. H., Calculation of Gauss quadrature rules, *Math. Comput.*, 23(106):221–230, 1969.
21. Gautschi, W., *Orthogonal Polynomials: Applications and Computations*, Oxford: Oxford University Press, 2004.
22. Delvos, F.-J., d-variate Boolean interpolation, *J. Approx. Th.*, 34:99–114, 1982.
23. Wasilkowski, G. W. and Woźniakowski, H., Explicit cost bounds of algorithms for multivariate tensor product problems, *J. Complexity*, 11(1):1–56, 1995.
24. Blatman, G., Adaptive sparse polynomial chaos expansions for uncertainty propagation and sensitivity analysis, Ph.D. Thesis, Université Blaise Pascal, Clermont-Ferrand, 2009.
25. Blatman, G. and Sudret, B., Adaptive sparse polynomial chaos expansion based on least angle regression, *J. Comput. Phys.*, 230(6):2345–2367, 2011.

APPENDIX A. GAUSS QUADRATURE AND ORTHOGONAL POLYNOMIALS

This Appendix develops only the orthogonal polynomial theory and Gauss quadrature theory needed for the EDO theory; derivation of the recursion relationships from the measure appear in Gautschi [21]. The abscissas, weights, as well as the convergence of Gauss quadrature with respect to a PDF $\mu(\xi)$ can be derived from an eigenvalue problem based on the recursion of the related orthogonal polynomials back to Golub and Welsch. Let $\mu(\xi)$ be a standard probability distribution over the interval I (namely Normal, $I = (-\infty, \infty)$, Gamma, $I = [0, \infty)$ or Beta distributions, $I = [0, 1]$). Here the orthogonal polynomials $P^j(\xi)$, $j = 1, 2, \ldots$ will be taken to be normalized

$$\int_I P^j(\xi) P^k(\xi) \mu(\xi) d\xi = \delta_{j,k} \tag{A.1}$$

where $\delta_{j,k}$ is the Kronecker delta. In this case $P^0(\xi) \equiv 1$ and the general recursion relation $k = 1, 2, \ldots$ can be written

$$\begin{aligned}(\alpha_0-\xi)P^0(\xi)+\beta_0P^1(\xi)&=0, \qquad k=0\\ \beta_{k-1}P^{k-1}(\xi)+(\alpha_k-\xi)P^k(\xi)+\beta_kP^{k+1}(\xi)&=0, \quad k>0\end{aligned} \tag{A.2}$$

Note that this can be summarized up to maximum order $N+1$ in the matrix equation

$$(\mathbf{J}-\xi\mathbf{I})\mathbf{P}=\begin{bmatrix}0\\ \vdots\\ 0\\ -\beta_{N-1}P^N(\xi)\end{bmatrix} \tag{A.3}$$

where $\mathbf{P}(\xi)=\left[P^0(\xi)\ P^1(\xi)\ \cdots\ P^N(\xi)\right]^T$, $\mathbf{I}$ is the N dimensional identity matrix, and $\mathbf{J}$ is the Jacobi matrix defined by

$$\mathbf{J}=\begin{bmatrix}\alpha_0 & \beta_0 & & & \\ \beta_0 & \alpha_1 & \beta_1 & & \\ & \beta_1 & \ddots & \ddots & \\ & & \ddots & \alpha_{N-2} & \beta_{N-2}\\ & & & \beta_{N-2} & \alpha_{N-1}\end{bmatrix}. \tag{A.4}$$

(Gautschi uses $\sqrt{\beta_n}$ on the off-diagonals.) This matrix has some very useful properties directly related to the polynomials. Note at the zeros $\xi^1<...<\xi^k<...<\xi^N$ of P^N, the (A.4) satisfies the eigenvalue equation

$$\left(\mathbf{J}-\xi^k\mathbf{I}\right)\mathbf{P}_k=0, \tag{A.5}$$

with eigenvector $\mathbf{P}_k=\mathbf{P}\left(\xi^k\right)=\left[P^0\left(\xi^k\right)\ P^1\left(\xi^k\right)\ ...\ P^{N-1}\left(\xi^k\right)\right]^{\mathrm{T}}$. In fact $\det\left(\mathbf{J}-\xi^k\mathbf{I}\right)=0$ for each k, and recursion to the N polynomial gives $\det\left(\mathbf{J}_N-\xi\mathbf{I}\right)=(-1)^N\beta_0...\beta_{(N-1)}P^N(\xi)$ and the roots of P^N are exactly the eigenvalues of $\mathbf{J}$. The eigenvectors of $\mathbf{J}$, $\mathbf{P}_1,\mathbf{P}_2,\ldots,\mathbf{P}_{N+1}$ are standardized to $[\mathbf{P}_k]_0=P^0\left(\xi^k\right)=1$. Since $\mathbf{J}$ in (A.4) is symmetric so that there is an orthogonal matrix $\mathbf{Q}$ which diagonalizes $\mathbf{J}$, $\mathbf{J}\mathbf{Q}^{\mathrm{T}}=\mathbf{Q}^{\mathrm{T}}\mathrm{diag}\left(\xi^1,\ldots,\xi^N\right)$, expressed with $\mathbf{Q}^{\mathrm{T}}$, a transpose of the usual form. (Technically, the rows of $\mathbf{Q}$ contain the left eigenvectors of $\mathbf{J}$). But such a $\mathbf{Q}^{\mathrm{T}}$ has eigenvectors columns, so that it must be that

$$\mathbf{Q}^{\mathrm{T}}=[w_1\mathbf{P}_1\ w_2\mathbf{P}_2\ \cdots\ w_N\mathbf{P}_N] \tag{A.6}$$

where $w_k=\|\mathbf{P}_k\|_2^{-1}=\left[\sum_{j=0}^N\left|P^j\left(\xi^k\right)\right|^2\right]^{-1/2}$ define the norming constants w_k for each eigenvalue ξ^k. The set of orders is $X=\{0,\ldots,N-1\}$ and the set of abscissa indices is $G=\{1,\ldots,N\}$. Define the linear operator $\mathcal{E}_G$ that evaluates function at the ξ^k and then weights the value as in (6) of Section 3.1. Then each column $\mathbf{Q}_k=\left[w_0P^k\left(\xi^0\right)\ \cdots\ w_NP^k\left(\xi^N\right)\right]^{\mathrm{T}}=\mathcal{E}_G\left(P^k\right)$ of $\mathbf{Q}$ contains all the weighted evaluations for single order polynomial P^k and is orthonormal compared to other rows, so that the orthonormality leads to

$$\sum_{j=0}^N w_j^2P^k\left(\xi^j\right)P^l\left(\xi^j\right)=\mathbf{Q}_k^{\mathrm{T}}\mathbf{Q}_l=\delta_{k,l}. \tag{A.7}$$

In particular for $l=k=0$, $\sum_{j=0}^N w_j^2=1$, so that the w_j^2 plays the discretized role of μ. The $\xi^1,\xi^2,...,\xi^{N+1}$ are the Christoffel abscissas (quadrature sample points) and w_k^2 are the Christoffel quadrature weights appropriate to the probability measure $\mu(\xi)$. Write the set of weights $W=\{w_k:k\in X\}$. Equation (A.7) states the orthonormality of the polynomials evaluated at the collocation points with respect to the weights. Restrict the dimensionality to finite polynomial set $\mathbb{O}_X=\left\{P^k:k\in x\right\}$ and $\mathcal{L}(\mathbb{O}_X)$ is the linear span of $\mathbb{O}_X$. Consider a function $f(\xi)\in\mathcal{L}(\mathbb{O}_X)=\mathbb{P}^N$, where $\mathcal{L}(\mathbb{O}_X)$ coincides with $\mathbb{P}^N$ the polynomials of order N. Then

$$f(\xi)=\sum_{j=0}^N c_jP^j(\xi). \tag{A.8}$$

Set $\mathbf{R} = \mathbf{Q}^{-1}$ (in this case $\mathbf{Q}^{-1} = \mathbf{Q}^{\mathrm{T}}$). The coefficients γ_j can now be found either by (A.1) or by (A.7) so that

$$c_k = \int_I f(\xi) P^k(\xi) \mu(\xi) d\xi = \sum_{j=0}^{N-1} w_j P^k\left(\xi^j\right) \phi_j = [\mathbf{R} W(F)]_k \tag{A.9}$$

where $\phi_j = w_j f\left(\xi^j\right) = [\mathcal{E}_G(F)]_j$ gives exactly the Gauss quadrature formula for polynomials. In general for $F = f + \epsilon(\xi)$

$$c_k = \int_I F(\xi) P^k(\xi) \mu(\xi) d\xi = [\mathbf{R}\mathcal{E}_G(f)]_k + O\left(\|\epsilon\|_2\right). \tag{A.10}$$

The Gauss quadrature error term $O\left(\|\epsilon\|_2\right)$ expresses convergence in terms of L^2 convergence with respect to probability measure p. If $\int \epsilon P^k \mu d\xi = 0$ for $k \in X$, the error is comparable to aliasing of the higher-order variability when sampling is effectively band-limited.

Sum up the properties in terms of notation from Section 3.1:

Gauss Quadrature for PC as EDO: $(G,\, X,\, \mathbf{R},\, W)$ is an EDO of $(I,\, X,\, \mathbb{O}_X,\, \mu)$, $f \in \mathcal{L}(\mathbb{O}_X)$, then f is uniquely reconstructed by (A.8) with $\mathbf{c}$ given by (A.9). The norm is preserved, $\|\mathbf{c}\|_{\mathbb{C}^N} = \|f\|_{L^2}$. Furthermore $\mathbf{R} = \mathbf{Q}^{\mathrm{T}}$ is unitary.

The unitarity means the condition number is 1. This is optimal as a start for fledging.

APPENDIX B. BOTTOM-UP FLEDGING PROOF

Suppose $\mathbf{Q}'$ is an invertible $M \times M$ sub-matrix of invertible $N \times N$ $\mathbf{Q}$, with $M < N - 1$. Only the induction step requires work and with the EDO theorem, this requires only that there is an invertible sub-matrix $\tilde{\mathbf{Q}}$ of $\mathbf{Q}$ of size $(M+1) \times (M+1)$ with $\mathbf{Q}'$ a sub-matrix of $\tilde{\mathbf{Q}}$. Without loss of generality, suppose $X' = \{1, \ldots, M\}$ and the columns of $\tilde{\mathbf{Q}}$ are $\tilde{X} = \{1, \ldots, M+1\}$. The proof uses the equivalence of invertibility with full rank in square matrices. Hence $\mathbf{Q}'$ is of rank M. The $\mathbf{Q}$ sub-matrix $\mathbf{Q}'' = [\mathbf{Q}'\mathbf{q}_1]$, with $(M+1) \times 1$ vector $[\mathbf{q}_1]_k = [\mathbf{Q}]_{k(M+1)}$, is also of rank M. Now the left $M+1$ columns of $\mathbf{Q}$, matrix, $\mathbf{Q}''' = \begin{bmatrix} \mathbf{Q}'' \\ \mathbf{Q}_2 \end{bmatrix}$, must be full rank $M+1$ since $\mathbf{Q}$ is full rank. Since $\mathbf{Q}''$ is row rank M there must be another row from $\mathbf{Q}_2$, as the remaining part of $\mathbf{Q}'''$, that is linearly independent of the rows of $\mathbf{Q}'$, say the $1 \times (m+1)$ row vector $\mathbf{q}_3$ with $[\mathbf{q}_3]_k = [Q]_{Jk}$ for appropriate j, $M < J \leq N$. Now $\tilde{\mathbf{Q}} = \begin{bmatrix} \mathbf{Q}'' \\ \mathbf{q}_3 \end{bmatrix}$ is full rank $(M+1) \times (M+1)$, and, hence, invertible.